Lehigh University
Lehigh Preserve

Theses and Dissertations

1990

Finite element study of fatigue characteristics of welded cover plate details

Mark R. Kaczinski
Lehigh University

Follow this and additional works at: https://preserve.lehigh.edu/etd

Part of the Civil Engineering Commons

Recommended Citation
Kaczinski, Mark R., "Finite element study of fatigue characteristics of welded cover plate details" (1990). *Theses and Dissertations*. 5415.
https://preserve.lehigh.edu/etd/5415

This Thesis is brought to you for free and open access by Lehigh Preserve. It has been accepted for inclusion in Theses and Dissertations by an authorized administrator of Lehigh Preserve. For more information, please contact preserve@lehigh.edu.

FINITE ELEMENT STUDY OF FATIGUE CHARACTERISTICS OF WELDED COVER PLATE DETAILS

by

Mark R. Kaczinski

A Thesis

Presented to the Graduate Committee

of Lehigh University

in Candidacy for the Degree of

Master of Science

in

Civil Engineering

Lehigh University

October 1990

CERTIFICATE OF APPROVAL

This thesis is accepted and approved in partial fulfillment of the requirements for the degree of Master of Science in Civil Engineering.

Oct 30, 1990
Date

Ben T. Yen
Professor in Charge

Irwin J. Kugelman
Department Chairman

ACKNOWLEDGEMENTS

The analytical study reported herein was conducted at Lehigh University's Department of Civil Engineering in conjunction with the Research Center for Advanced Technology for Large Structural Systems (ATLSS). Dr. Irwin J. Kugelman is chairman of the Civil Engineering department and Dr. John W. Fisher is Director of the ATLSS Center. This work was part of a larger experimental research program on "Fatigue Behavior of Welded Aluminum Components" being sponsored by the Aluminum Company of America (Alcoa).

The author is sincerely indebted to Dr. Ben T. Yen who was both a thesis supervisor and friend, as well as Craig C. Menzemer who straddled the line between being the Alcoa project liason and a fellow graduate student. Without their support and guidance this work would not have been possible.

Special thanks go to my wife, Mary, for providing the encouragement necessary to join her in making the jump back into the academic world and also for her support over the last two years.

TABLE OF CONTENTS

Abstract	1
1. Introduction	3
1.1 History of Fatigue Cracking at Cover Plate Details	3
1.2 Linear Elastic Fracture Mechanics	4
1.3 Objective and Scope of Study	6
2. Finite Element Model	9
2.1 Three-Dimensional Beam Model	9
2.2 Two-Dimensional Models	13
3. Stress Intensity Factors	16
3.1 Energy Release Rate Method	16
3.2 Green's Function Method	19
3.3 Results	23
4. Fatigue Life Prediction	25
4.1 Paris Power Law	25
4.2 Results	27
5. Parametric Study of Cover Plate Geometry	30
5.1 Geometric Parameters	31
5.2 Results	31
5.3 Comparison to SPATE Results	32
6. Summary and Conclusions	34
Tables	36
Figures	39
References	58
Vita	60

LIST OF TABLES

Table 1 - Stress Intensity Factors by the Energy Release Rate Method 36

Table 2 - Calculated S-N Data Points 37

Table 3 - Stress Concentration Factors 38

LIST OF FIGURES

Figure 1 -	Beam Geometry	39
Figure 2 -	Elevation of 3-D Finite Element Mesh	40
Figure 3 -	Cross Section of Finite Element Mesh	41
Figure 4 -	Beam Flange Stress Distribution along Web Centerline	42
Figure 5 -	Influence of Mesh Size on Maximum Stress	43
Figure 6 -	Partial Histogram of Welded Joint Defect Sizes	44
Figure 7 -	Finite Element Submodel 1	45
Figure 8 -	Finite Element Submodel 2	46
Figure 9 -	Finite Element Submodel 3	47
Figure 10 -	Finite Element Submodel 4	48
Figure 11 -	Finite Element Nodes near Crack Tip	49
Figure 12 -	Correction Factor Variation with Crack Depth	50
Figure 13 -	Calculated Stress Intensity Factors for Tension Specimen	51
Figure 14 -	Stress Intensity Factor Variation with Specimen Type	52
Figure 15 -	Fatigue Crack Propagation Curve	53
Figure 16 -	Generated S-N Curve for Beam Specimen	54
Figure 17 -	Generated S-N Curve for Tension Specimen	55
Figure 18 -	Combined S-N Curves	56
Figure 19 -	Stress Concentration Factor Variation	57

ABSTRACT

Fatigue strength characteristics of full-scale welded steel cover plate details have been studied extensively since the 1960's and therefore can be accurately predicted. However, research on welded full-scale aluminum details, including the cover plate, is limited and an experimental program is currently underway to establish a more comprehensive understanding of their behavior. The principle objective of this thesis is to develop an analytical model of fatigue crack propagation and life prediction at aluminum cover plate details for both axially loaded tension specimens and full-scale beam specimens.

Albrecht and Yamada's simplified procedure to calculate stress intensity factors produces results which compare closely with upper-bound solutions and is used exclusively in this study. Using these K values and crack growth rates for aluminum alloy 5456-H116, analytical S-N curves are calculated which agree with cover plate fatigue test data. Tension specimen details exhibit fatigue lives 40% higher than those of comparable beam specimens. It is also evident that the cover plate orientation affects fatigue life. Beam specimens with cover plates extending from each end of the beam towards midspan, as in current test specimens, have a predicted life expectancy 14% higher than a conventionally oriented detail at the same nominal stress.

A parametric study is conducted on cover plate details to study the effect of geometry on the stress concentration factor by varying flange thickness, cover plate thickness, and weld size. The results indicate that the fatigue strength of these details is a function of more than flange thickness. Finally, recommendations for future studies are proposed.

CHAPTER 1 - INTRODUCTION

1.1 History Of Fatigue Cracking at Cover Plate Details

The problem of fatigue, crack propagation which may lead to failure of components at stresses below their yield point when subjected to cyclic loading, was first studied by Wohler[1] over a century ago. His work on railway axles introduced the concept that stress concentrations exist at abrupt changes in section geometry and that these details will then reduce the components resistance to cyclic loading. The focus of all early fatigue research was on machinery parts and riveted connections.

Large scale fabrication of welded steel beams began in the 1950's and within a decade localized failures were occuring on steel bridge components due to fatigue. The stress distribution at welded structural details is influenced by two independent sources of stress concentration. Inherent geometric discontinuities at all structural details produce a non-uniform stress distribution without any flaws or cracks being present. In addition, the welding process was found to frequently create discontinuities such as porosity, inclusions and incomplete fusion which act as a localized stress concentration. If these flaws remain undetected, they provide an initiation site for fatigue cracking when they are oriented perpendicular to the applied stresses. In the 1960's, the welded cover plate detail was first recognized as having poor fatigue resistance. This was first apparent during the AASHO

Road Test program[2] when cover plate details began cracking with as little as 500,000 vehicle crossings. Soon afterward, one of the first documented cases of cracked bridge details occured at the Yellow Mill Pond Bridge located at Bridgeport, Connecticut[3]. An extensive number of fatigue cracks were discovered in 1970 on this simple span structure at the termination of cover plates on the tension flange.

When the AASHTO fatigue specifications[4] were first adopted in 1974, cover plate details were classified as Category E. This category had the lowest fatigue strength of all structural details with an allowable stress range of 5 ksi when more than 2 million load cycles are expected. Additional research[5] and several service failures indicated that even this limit was unconservative for some situations. Current fatigue codes (AISC[6] and AASHTO[7]) specify that cover plate details be classified as either Category E or E′ depending on the flange thickness. The Category E fatigue strength remains at 5 ksi while the Category E′ strength is reduced to 2.6 ksi when the flange thickness is greater than 0.8 inches.

1.2 Review of Linear Elastic Fracture Mechanics

It is generally accepted that all fabricated structural members contain defects. Proper design recognizes the presence of these defects and minimizes the probability of cracking. Linear elastic fracture mechanics (LEFM)[8] is a tool used to characterize the load-carrying capacity and durability of members with flaws.

LEFM provides an analytical procedure which relates the stress field intensity in the vicinity of a crack to the nominal stress in the member and the size, shape, and orientation of the crack or crack-like discontinuity. This quantitative measure of a crack's severity is called the stress intensity factor - K. The development of LEFM in the 1950's greatly expanded the understanding of stable crack extension (fatigue) and crack instability (fracture). An understanding of both the fatigue and fracture phenomena is critical for the fail-safe design of structural components.

Use of LEFM to solve engineering problems requires calculation of the stress intensity factor. The stress intensity factor can always be expressed in general terms as

$$K = CF \times \sigma \sqrt{\pi a} \tag{1-1}$$

where CF = Correction Factor
σ = Nominal member stress
a = Crack length.

For the idealized situation of a central, through-crack in an infinite plate, the correction factor (CF) equals 1.0. Closed form analytical solutions for CF also exist for many other geometrical conditions and can be found in Handbooks[9]. However, for many complex welded details such as cover plates, handbook solutions are unavailable and numerical solutions must be obtained.

Of all numerical methods, a finite element analysis usually leads to acceptable results and provides the most versatility. Any geometrical configuration, regardless of

complexity, which may be accurately modelled by finite element methods can be solved to find the stress intensity factor. For this report, the finite element technique is used to solve for K at cover plate details by two different methods. Each method is discussed in detail and the results compared in Chapter 3.

1.3 Objective and Scope of Study

The work presented in this report is part of a larger study on "Fatigue Behavior of Welded Aluminum Components" being sponsored by the Aluminum Company of America (Alcoa) at the Center for Advanced Technology for Large Structural Systems (ATLSS) at Lehigh University. Current aluminum fatigue specifications are based on test results of small scale tension specimens and much of this data remains unpublished as it was privately produced. Work to develop a comprehensive specification based on results of large scale beam specimens was started by Kosteas at the Technical University of Munich in the early 1980's. Results from the current Alcoa project will supplement Kosteas' work and be added to the expanding data base on fatigue of aluminum weldments.

The principle objective of this study is to develop an analytical model of fatigue crack propagation and life prediction at aluminum cover plate details for both axially loaded tension specimens and full scale beam specimens. A three-dimensional model of the test beam and several two-

dimensional submodels are developed and analyzed assuming linear elastic behavior by the finite element program ADINA[10].

Using finite element techniques, K is calculated for the detail by two different methods. The first method is a compliance analysis which involves analyzing the detail repeatedly with varing crack lengths. Energy Release Rate, G, is calculated from the results of the analysis at each crack length[11], and this value can then be directly related to K by LEFM. The second method consists of expanding on the accepted solution for the stress intensity factor of Equation 1-1 by including a modification factor in CF to account for the detail's geometry[12]. This geometric correction factor (F_G) is obtained using a Green's function to represent the splitting forces at the crack and then integrating away the normal stress along the crack path. Only one finite element computation is required on the as-fabricated detail to determine the stress gradient along the predicted crack path.

S-N curves are developed for both the tension and beam specimens from the K solutions, crack growth data and initial flaw size information. These curves are compared to fatigue data points as a method of validating the life prediction model. Another check on the finite element model results is obtained by comparing stress concentration values at the toe of the fillet weld by finite element analysis and full field stress measurements using the SPATE technique.

Two other topics are also investigated. First, models of two-dimensional, axially loaded tension specimens are used to

study the effects of cover plate geometry on the stress concentration factor (SCF). Flange and cover plate thickness, as well as fillet weld size are varied to determine their effect on the stress concentration at the weld toe. Secondly, the effect of cover plate orientation on fatigue life is examined. Recent fatigue testing programs have used beams with cover plates which extend from each end of the beam towards midspan. However, a cover plate on a conventional simple span beam would extend through the midspan region and terminate some distance from the ends of the beam. Although this modification does not change the nominal stress at the detail, the beam curvature (M/EI) diagram is altered.

The five remaining chapters of this report consist of the following. Chapter 2 describes the finite element models used for the analytical study. An explanation of the two methods used to calculate K, as well as results are presented in Chapter 3. Chapter 4 explains the calculation of fatigue life prediction values for both beam and tension specimens and also includes comparisons to test results. The results of a parametric study on the effect of cover plate geometry on SCF's is presented in Chapter 5. Finally, a comprehensive summary is included in Chapter 6.

CHAPTER 2 - FINITE ELEMENT MODEL

The cover plate detail is difficult to analyze because of the three-dimensional stress field which exists at the toe of the transverse fillet weld joining the cover plate and flange. To effectively model the detail to observe this behavior would require multiple layers of through-thickness, 8-node brick elements from the ADINA[10] element library. Such a model could require an excessive number of degrees-of-freedom and therefore, make the finite element problem both cumbersome and cost prohibitive. To solve this problem, the method of submodelling is used. This procedure involves application of the necessary loads to a coarse 3-D mesh. Next, a finer two-dimensional mesh with planar elements is analyzed with displacement input from the 3-D mesh results. Then three successively finer 2-D meshes with planar elements are analyzed with displacement input from each previous submodel. This submodelling procedure has the advantage that no one model becomes excessively large and also provides the opportunity to reuse two of the 2-D models in a parametric study of cover plate geometry.

2.1 Three-Dimensional Beam Model

The 3-D model is a coarse mesh which is used to obtain the global behavior of the beam adjacent to the cover plate detail. The beam geometry modelled is similar to that of the full-scale welded aluminum beams being tested by Alcoa at the

ATLSS center. Each built-up beam spans 15 feet and is fabricated from 1 in. x 12 in. flange plates and a 1/2 in. x 16 in. web plate. The cover plates are 5/8 in. x 9 in. and on the test beam configuration extend 39.5 inches from the beam end reaction. For the conventional beam model, 5/8 in. x 9 in. plates are again used as cover plates, however they extend through the midspan region and terminate 39.5 inches from the beam end reaction. Partial depth 3/8 in. stiffener plates are located under the two load points resulting in a four point loading configuration. While the loading stiffeners are modelled, the full depth stiffeners are not. Figure 1 is a sketch of the beam section being tested and modelled. Figure 2 shows elevation views of the 3-D beam mesh with cover plates oriented in both the test and conventional orientation. Cross sections of each are shown in Figure 3. The material is considered to be linear, isotropic and homogeneous - including the weld region - with a Young's modulus (E) and Poisson's ratio (v) of 10,300 ksi and 0.28 respectively. These material properties are typical of structural aluminum alloys, and in this case represent 5456-H116.

The 3-D finite element mesh consists of a variety of ADINA elements. Advantage is taken of double symmetry to reduce the mesh size and computational effort by cutting the beam along both the midspan and longitudinal centerlines. Three-diminsional 8-node brick elements are used to model the tension flange and cover plate. One element is used through the thickness of each plate. Maximum aspect ratios of 1.5:1.0

and 2.4:1.0 for the flange and cover plate are below recommended modelling guidelines. As only the global behavior is of interest at this stage, the fillet weld connecting the flange and cover plate is neglected. Because of this decision, the flange and cover plate elements are connected along all common nodes and is not representative of the actual condition away from the weld fusion zone. However, such an approximation does not significantly effect the stiffness of the model and should have little or no influence on the displacement input to the first substructure. All brick element nodes along the longitudinal beam centerline have translations in the x-direction prevented to provide symmetry along this axis.

The beam web is modelled with 4-node plane stress elements of 1/4 in. thickness. These elements are typically rectangular and have an aspect ratio of 1.1:1.0 away from the web-flange transition zone. The x-direction (out-of-plane) translations are prevented to conform to the 2-D behavior of the element and insure symmetry along the longitudinal beam axis. Beam elements, typically 5 in. long, are used to model the compression flange and cover plate. Each element has the x-direction translation and out-of-plane rotational degree-of-freedom supressed. Additional boundary conditions used to model the simple span beam with double symmetry include y-direction or vertical rollers at all nodes along the midspan centerline and a single z-direction or horizontal roller at the end of the beam span.

An arbitrary 10 kip load is applied to the model by nine concentrated vertical nodal loads across the tension flange, 59 inches from the end reaction. The magnitude of the load can be arbitrary since all results will be either relative to (i.e. K_I) or normalized by (i.e. SCF) the resultant nominal stress at the detail. However, due to the double symmetry of the model the actual load being applied to the beam is four times this value or 40 kips. To reduce localized bending of the flange adjacent to the applied concentrated loads, the tension flange has been stiffened by two methods. In addition to the partial depth stiffener directly under the load, three rows of rigid beam elements are placed across the tension flange adjacent to the concentrated loads.

To make the transition between three- and two-dimensional meshes, it is necessary to select a vertical plane to cut out along the flange for further investigation. As in previous work by Albrecht[12] and Zettlemoyer[13] the vertical plane to be considered two-dimensionally is along the web line (at x=0). Due to shear lag considerations this plane would have the highest stress concentrations and therefore yield conservative results. The borders of this cut are selected at locations sufficiently away from the cover plate termination where the stress distribution is uniform through the flange and cover plate. Figure 4 shows the stress distribution along the tension flange and border locations for the beam with a test cover plate orientation. Nodal point displacements, both vertical (y-direction) and horizontal (z-direction), through

the flange and cover plate at the borders and along the web-flange intersection between these borders will be used as displacement input for the two-dimensional model.

2.2 Two-Dimensional Models

Four planar 2-D meshes are developed as submodels for the beam specimens. The decision to use plane stress or plane strain elements is dependent on the detail geometry. Plane strain elements are used in all meshes because they best represent the lateral constraint provided in the out-of-plane direction of the flange and cover plate. The actual condition at the detail is a combination of plane strain behavior within the plate material and plane stress behavior at the surfaces. However, work by Zettlemoyer has shown that the decision to use plane stress or strain elements results in small differences and hence is not overly important. This is especially true if the detail geometry is considered by first performing a 3-D analysis.

Past fatigue failures and research have shown that the critical location for a properly designed and fabricated cover plate detail is the fillet weld toe. It is the stress at this location and the stresses along the crack path which will be investigated. For simplicity, the crack path will be assumed to travel perpendicularly from the extreme fiber of the tension flange through the plate thickness at the weld toe. In the finite element model, the fillet weld is assumed to project at 45 degrees from the flange with a leg dimension of

0.4 inches. The sharp geometric change created at the weld toe causes a global stress concentration to occur. It has been shown that this stress concentration will increase as the weld angle increases[14] and theoretically will approach infinity when the angle is 90 degrees. Hence, the assumption of a 45 degree weld angle is important. Because of this stress concentration, mesh size adjacent to the weld toe becomes an issue when an elastic analysis is performed. It can be seen from Figure 5 that as the mesh size decreases, the stress concentration will increase. Just how small should the mesh be was addressed by Zettlemoyer who determined that to ensure reasonable accuracy the mesh size in the vicinity of the weld toe should not exceed the initial crack size - a_i. Since the majority of reported initial flaw sizes at aluminum details[15] is 0.0005 in. to 0.001 in. as illustrated in Figure 6, a mesh consisting of 0.001 in. x 0.001 in. elements adjacent to the fillet weld toe is utilized for the final model.

No global boundary conditions are placed on the submodels as y and z displacements from either the 3-D global model or subsequent 2-D submodels are used as input along all cut boundaries. Since each submodel mesh is finer than the previous, linear interpolation of both displacements are applied at all new nodes. Figures 7 to 10 show overall mesh dimensions and element sizes for submodels 1 through 4. The size of submodels 2 to 4 are determined by examination of the stress distribution along the top of the flange of the

previous model. A length is chosen outside of the zone affected by the stress concentration at the toe of the fillet weld.

For the parametric study of cover plate geometry, submodels 2 and 4 are utilized. Submodel 4 is unchanged, while submodel 2 is modified to allow application of concentrated loads and variations in flange and cover plate dimensions. Submodel 3 is unecessary in the modelling of tension members because of the lack of a gradient in the flange stresses. Nodal loads are applied along the right boundary of the model to produce a 10 ksi nominal stress in the flange. Equilibrium of the system is maintained by preventing y and z translations at all flange and cover plate nodes along the left boundary. Flange and cover plate thickness parameters are discussed in Chapter 5.

Chapter 3 - STRESS INTENSITY FACTORS

Stress intensity factors are calculated for the cover plate detail by two approximate methods employing finite element techniques coupled with linear elastic fracture mechanics. Because of its simplicity and reduced computer requirements, the Green's function method is used as the primary solution technique for K in this report. As a comparative study, stress intensity factors for the tension specimen model are calculated by both the Energy Release Rate and Green's function method. However, only the Green's function method is used to calculate K for each of the beam specimen models. Each method and the results are described below.

3.1 Energy Release Rate Method

The Energy Release Rate method is a compliance analysis which involves analyzing the cover plate detail with multiple crack lengths. A finite element analysis is used to determine the energy release rate, G, from which stress intensity factors can easily be calculated. Several methods are available in the literature to evaluate G through finite element techniques. In this report, the energy release rate is calculated by computing the crack closure integral as presented by Rybicki in Reference 11.

Irwin[16] believed that if a crack extends by a small amount Δc, the energy absorbed in the process is equal to the

work required to close the crack to its original length. This statement can be expressed in equation form for uncoupled Mode I and Mode II deformations as follows:

$$G_I = \lim_{\Delta c \to 0} \frac{1}{2\Delta c} \int_0^{\Delta c} \sigma_z(\Delta c - r, 0)\ \overline{w}(r, \pi)\, dr \qquad (3\text{-}1)$$

$$G_{II} = \lim_{\Delta c \to 0} \frac{1}{2\Delta c} \int_0^{\Delta c} \tau_{yz}(\Delta c - r, 0)\ \overline{v}(r, \pi)\, dr \qquad (3\text{-}2)$$

A polar coordinate system with the origin at the crack tip is used and σ_z and τ_{yz} are stresses near the crack tip, $\overline{w}$ and $\overline{v}$ are the relative opening (Mode I) and sliding (Mode II) displacements on the crack face, and Δc is the crack extension length. Although this method permits the calculation of both K_I and K_{II}, only Mode I stress intensity factors are determined. Solutions for K_I are considered to be of primary importance for civil engineering structural fatigue problems.

The integral in Equation 3-1, which represents the amount of work required to close the crack an amount Δc, must be modified to accept the nodal force and displacement results of each finite element analysis. Work required to close the crack, in terms of finite element results, is defined as one-half the product of the forces at c and d required to close these nodes. Figure 11 helps to illustrate this procedure. A modified expression for G_I can be stated as

$$G_I = \lim_{\Delta c \to 0} \frac{1}{2\Delta c} \overline{F}_c (w_c - w_d) \tag{3-3}$$

where $\overline{F}_c$ is the z-force required to hold nodes c and d together. The force at the crack tip, $\overline{F}_c$, is obtained by placing a very stiff truss element between nodes e and f and determining its axial force. This procedure for obtaining $\overline{F}_c$ is valid only when ℓ_2 equals Δc and elements 1, 2, 3 and 4 are of the same size. For cases when ℓ_2 is not equal to Δc, $\overline{F}_c$ is estimated by the equation

$$\overline{F}_c = \left(\frac{\Delta c}{\ell_2}\right)^{\frac{1}{2}} F_e \tag{3-4}$$

where F_e is the axial load in the truss element between nodes e and f.

The relationship between G_I and K_I is established by subtituting Westergaard's representations for the stresses and displacements near a crack into Equation 3-1 and solving. The result is

$$G_I = \frac{K_I^2}{E} (1-\nu) \tag{3-5}$$

under plane strain conditions.

This procedure yields results within 6% of reference solutions when the crack length is at least five times greater than Δc. Applying this limitation to finite element submodel mesh 4, with 0.001 in. × 0.001 in. elements adjacent to the weld toe, the shortest crack length which can be analyzed is 0.005 inches. Stress intensity factors are also determined

for crack lengths of 0.010, 0.020, 0.050, 0.100 and 0.200 inches in submodel 4 when an uncracked analysis is performed on submodel 2.

Computer runs are also performed with crack lengths of 0.05, 0.100 and 0.200 inches in both submodel 2 and 4. The stress intensity factors calculated by this procedure may be considered as upper-bound solutions because of the secondary bending effects introduced by a large crack in submodel 2 which would not be present in the actual global behavior of the beam. This case is referred to as a cracked global condition.

Calculated stress intensity factors for the tension specimen cover plate detail with various crack lengths are listed in Table 1. The solutions from both cracked and uncracked global stress analysis appear to converge at short crack lengths. However, as the crack length and secondary bending effects increase, the difference in results becomes quite large. For example, with a crack length of 0.200 inch the stress intensity factors for the uncracked and cracked global condition are 5.9 and 9.4 ksi$\sqrt{\text{in}}$ respectively.

3.2 Green's Function Method

The Green's function method, as it is referred to in this report, is based on Albrecht and Yamada's procedure[12] to calculate stress intensity factors. This method is based on Irwin's idealized equation,

$$K = \sigma\sqrt{\pi a} \tag{3-6}$$

which calculates the stress intensity factor of a centrally through-cracked infinite plate subject to a uniform distributed crack opening stress. However, to apply this equation to real cracked details requires modification into

$$K = CF \times \sigma\sqrt{\pi a} \tag{3-7}$$

which includes a correction factor (CF) to account for detail geometry, crack shape and distribution of applied stresses. Using this method only one uncracked finite element analysis is necessary to calculate K values for any crack size at the most complex details. Due to geometric discontinuities at the weld toe of cover plate details, the stress distribution is non-uniform and the correction factor in Equation 3-7 must include a term to account for these geometric effects.

This geometric correction factor (F_G) is included in CF of Equation 3-7 which can be expressed as

$$CF = F_G \times F_W \times F_S \times F_E \tag{3-8}$$

In addition to F_G, modifications are also made to account for finite width F_W, free surface effects F_S, and elliptical crack fronts F_E. The number of available modification factors is greater than these four, however, they are the most important for solving practical fatigue and fracture problems.

The geometric correction factor, F_G, is obtained by using a Green's function to represent the non-uniform splitting forces at the crack and then integrating away the normal

stress along the anticipated crack path. This factor is equal to

$$F_G = \frac{2}{\pi} \sum_{i=1}^{n} \frac{\sigma_{bi}}{\sigma} \left(\arcsin \frac{b_{i+1}}{a} - \arcsin \frac{b_i}{a} \right) \tag{3-9}$$

where:
- a = Crack length
- b = Discrete distance from extreme fiber of flange to finite element stress location
- σ = Nominal normal stress at detail computed by strength of material formulas
- σ_{bi} = Finite element normal stress along crack path

for stress distributions obtained by finite element methods.

A free surface correction of

$$F_S = 1.211 - 0.186 \sqrt{\frac{a}{c}} \tag{3-10}$$

is used to account for a semi-elliptical edge crack with minor and major semi-axis lengths of (a) and (c) respectively.

The correction factor for a central crack in a finite width plate, W, is frequently approximated by the equation

$$F_W = \left(\frac{W}{\pi a} \tan \frac{\pi a}{W} \right)^{\frac{1}{2}} \tag{3-11}$$

This equation can be modified to also handle the situation of an edge crack growing through the plate thickness by replacing W with two times the plate thickness (2T).

At the point on the ellipse of maximum stress intensity ($\phi = \pi/2$) the elliptical crack shape correction factor is simplified to

$$F_E = \frac{1}{E_K} \tag{3-12}$$

This situation generally exists at beam flange details where the primary stress is uniform tension and the a/c ratio of the crack is below 0.80. Calculation of E_K involves solving

$$E_K = \int_0^{\frac{\pi}{2}} (1 - K^2 \sin^2\theta)^{\frac{1}{2}} \, d\theta \tag{3-13}$$

for the complete elliptical integral of the second kind. Fortunately, there exists a simplification of this equation in the form

$$E_K = \sqrt{Q} \tag{3-14}$$

where

$$Q = 1 + 1.464\left(\frac{c}{a}\right)^{1.65} \qquad For \quad \frac{a}{c} < 1$$

or (3-15)

$$Q = 1 + 1.464\left(\frac{a}{c}\right)^{1.65} \qquad For \quad \frac{a}{c} > 1$$

which is valid only for the location of maximum K[17].

Each of the modification factors are derived with the assumption that no interaction exists between the four effects and this leads to the introduction of some degree of uncertainty in problems when all the factors must be combined. However, the level of inaccuracy has been proven to be low when values calculated by this method are compared to test results. This is particularly true when the stress distribution away from the cracked detail is one of uniform

tension. For cases where a non-uniform stress distribution exists, more complex methods (i.e. Energy Release Rate) should be used since Mode II or Mode III crack opening displacements may be dominant and may not be solved by the Green's function method.

Relationships between the minor (a) and major (c) axis semidiameters have been empirically determined for steel cover plate details[18]. The lower bound equation

$$c = 5.451 a^{1.133} \tag{3-16}$$

is used to simplify equations 3-10 and 3-15 in terms of only the crack length - a. A short computer program is used to calculate F_G using results of the finite element analysis. This program also determines F_W, F_E and F_S values, as well as K_I for the cover plate detail with crack lengths of 0.001 in to 0.475 inches. The four correction factors and resulting stress intensity factor for the tension specimen are plotted in Figures 12 and 13 respectively. For comparative purposes, Figure 13 also contains values of K_I determined by the Energy Release Rate method.

3.3 Results

Stress intensity factors for the tension specimen calculated by both the Energy Release Rate and Green's function method are plotted in Figure 13. It can be seen that the Green's function results are in very close agreement with those of the Energy Release Rate method for a cracked global condition. The Green's function method produces a

conservative upper-bound solution for K when a lower-bound a/c relationship is assumed to describe the crack geometry at the cover plate detail. Therefore, this relatively simple and inexpensive method is used exclusively to calculate K for the beam specimen models with both cover plate orientations.

Stress intensity factors for both beam specimen models and values for the tension specimen model are compared in Figure 14. The beam model with a conventional cover plate orientation yields K values consistently higher than those of a test cover plate orientation. The significance of this difference in K can be most effectively studied by life prediction estimates.

From Figure 14 it can also be seen that both of the beam specimen results are higher than those of the direct tension specimen for crack lengths less than 0.35 inches. This is probably due to the additional crack opening displacements and resulting stress gradient produced by bending in the beam flange. Again, the relative difference in K between specimen types can best be compared by life prediction estimates.

Chapter 4 - FATIGUE LIFE PREDICTION

Fatigue life is calculated to develop analytical S-N curves for the aluminum cover plate details. As a check on model validity, the results for a beam specimen with a test cover plate orientation and tension specimen are compared to fatigue data points. For comparative purposes, an S-N curve of the beam specimen with a conventional cover plate orientation is also calculated. The Paris Power Law is used to predict fatigue life.

4.1 Paris Power Law

Although many methods of calculating fatigue life can be found in the literature, it is the Paris Power Law which is most widely accepted[19]. Paris, who considered only crack propagation in life calculations, recognized that crack growth per cycle, da/dN, can be empirically related to K from linear elastic fracture mechanics by

$$\frac{da}{dn} = C(\Delta K)^n \tag{4-1}$$

where $\Delta K = K_{max} - K_{min}$ and C and n are material properties. Equation 4-1 is limited to Zone II of the sigmoidal shaped fatigue crack propagation curve shown in Figure 15. However, for welded details the inherent flaws due to fabrication eliminate the initiation stage (Zone I) of fatigue crack growth and in most cases can be ignored in fatigue life calculations. Also, the contribution of Zone III on fatigue

life is negligible because crack growth approaches the stability limit point. The Paris equation will therefore yield acceptable predictions of the fatigue life of many common structural details.

By rearranging equation 4-1 and numerically integrating between the initial (a_i) and final (a_f) crack sizes, the number of cycles can be predicted as:

$$N = \frac{1}{C} \sum_{j=1}^{m} \frac{1}{(\Delta K_j)^n} \Delta a_j \qquad (4\text{-}2)$$

where $C=6.436\times10^{-9}$ and $n=3.098$ when units of inches are used for crack length and ksi$\sqrt{in}$ for ΔK. These material property constants are extrapolated from recent results of fatigue crack growth (FCG) tests conducted on 1 inch thick 5456-H116 aluminum specimens[15]. A power fit regression analysis is used to obtain solutions for the dominant C and n values in the Zone II region.

Fatigue life values are calculated as the number of cycles required to propagate a crack to a depth of 0.475 inches in the flange. This value for a_f is a limitation of the finite element analysis, and although it may not be a through-thickness crack, it accurately predicts failure at the detail. Crack lengths beyond 0.475 in. produce rapidly increasing stress intensity factors near the material toughness limit (Zone III) which will trigger crack instability (fracture). Even more important than the choice of a_f is the estimated initial crack size which has a much stronger influence on the fatigue life. The smallest a_i which can be assumed is 0.001

in. and is representative of the majority of observed flaw sizes in micrographs of fractured specimens[15]. A lower bound life prediction is also found by assuming a_i to equal 0.006 inch.

A simple computer program is used to calculate the number of cycles required for the crack to propagate from each value of a_i to 0.475 inch. The calculated life for each specimen at nominal stress ranges of 2.9, 4.1 and 5.8 ksi are listed in Table 2. These three stress ranges correspond to the actual nominal stress in cover plate details tested at Lehigh University.

4.2 Results

From the results in Table 2, it can be seen that small increases in the initial flaw size will significantly reduce the number of cycles to failure. Fatigue life of the welded aluminum cover plate detail is reduced by 13-15% when the initial flaw size is increased from 0.001 inch to 0.006 inch. This reduction is independent of stress range, specimen type and cover plate orientation.

Figures 16 and 17 are plots of the analytically developed S-N curves and actual fatigue data points for the beam and tension specimens respectively. For each specimen type, the predicted S-N curve slopes approximately parallel to the limited test data. A lower bound life prediction is obtained for tension specimens when an initial flaw size of at least 0.001 inch is assumed. Test results of beam specimen cover

plate details are scattered both above and below the S-N curve and its location appears to predict the mean fatigue life. The results for each specimen type are accurate enough to closely predict fatigue life of cover plate details and to determine that the analytical model was developed adequately.

In Figure 18 results for the beam and tension specimens are combined. From these results, it can be calculated that the predicted life expectancy of a tension specimen is 25% greater than that of a beam specimen with a test cover plate orientation. A 40% increase is also predicted for the tension specimen relative to beam specimens with a conventional cover plate orientation. Test results of small scale axially loaded aluminum specimens which exhibit up to 40% higher fatigue strengths than their full-scale beam counterparts have been previously reported in the literature[20]. This descrepancy is believed to be caused by differences in residual stresses due to size effects. However, since residual stresses are not included in this analytical model another factor must be contributing to the difference in results. One source is the stress gradient through the flange thickness produced by bending.

From the results in Table 2, it can also be seen that the cover plate orientation does indeed affect fatigue strength. Beam specimens with cover plates oriented for testing unconservatively overestimate fatigue life of conventionally cover rated beams by 14%. This difference should be

considered in future test programs which use beams fabricated with non-conventional cover plate orientations.

Chapter 5 - PARAMETRIC STUDY OF COVER PLATE GEOMETRY

A finite element parametric study is conducted on cover plate details to study the effect of geometry on the stress concentration factor (SCF). Flange thickness, cover plate thickness, and weld size are varied and the models are analyzed as two-dimensional axially loaded tension members to reduce the computational effort. Even though flange stresses in the tension model are a simplification of stresses in a three-dimensional beam, relative changes in SCF due to geometric variations can be studied effectively.

It has been well known since the work of Wohler that stress concentration plays a very important role in the fatigue strength of structural details and today is the basis for distinguishing the various AASHTO fatigue categories. In this report, SCF is defined as the extreme fiber stress in the flange at the toe of the fillet weld divided by the nominal stress in the member. For an axially loaded tension member the nominal stress is simply the axial load divided by the cross sectional area at the location being studied.

This work is an expansion of that done by Zettlemoyer in 1976 and intends to expand into the more practical range of flange to cover plate thickness ratios for currently fabricated cover plated beams. Only two of the five models analyzed by Zettlemoyer contain the more common geometrical condition where flange thickness is greater than the cover plate thickness.

5.1 Geometric Parameters

The two geometric parameters included in this study are the flange to cover plate thickness ratio (T_F/T_{CP}) and the weld leg size to cover plate thickness ratio (W/T_{CP}). Two W/T_{CP} ratios are studied, 0.64 and 0.80, which requires two slightly different finite element models. For W/T_{cp} = 0.64, the model used is that of submodels 2 and 4 from the analysis of beam specimens with a 0.4 in. fillet weld. The cover plate thickness is kept constant at 5/8 in. and flange thicknesses of 5/8, 1.0 and 1 7/8 inches are modelled to analyze T_F/T_{CP} ratios of 1.0, 1.6 and 3.0 respectively.

For W/T_{CP} = 0.80, submodels 2 is geometrically modified to include a 1/2 in. cover plate with a 0.4 in. fillet weld. Six T_F/T_{CP} ratios are studied by modelling flange thicknesses of 0.5, 0.7, 1.0, 1.3, 1.5 and 2.0 inches.

To limit the number of independent variables in the study the weld angle is kept constant at the idealized condition of 45 degrees. It should be recognized that changes in this angle will increase or decrease both SCF and K for the detail[14].

5.2 Results

Table 3 lists the SCF values for each combination of geometrical parameters studied. These results are also plotted in Figure 19 which shows that SCF will increase as the T_F/T_{CP} ratio increases and as the W/T_{CP} ratio decreases. For

either W/T_{CP} ratio, the rate of change of SCF is greater at low T_F/T_{CP} ratios and tends to asymptotically approach a limit at higher ratios. This is contrary to the constant 6-8% increase in SCF at all T_F/T_{CP} values when the W/T_{CP} ratio is reduced by 29% from 0.80 to 0.64. From these results it appears that SCF and hence fatigue life of cover plate details is a function of more than just flange thickness as currently specified by AASHTO. In fact, the transverse fillet weld size at the cover plate termination is at least as important as flange thickness in affecting SCF at lower T_F/T_{CP} ratios and possibly more important at higher ratios.

The equation

$$SCF = 5.798 + 1.981 \log\left(\frac{T_{CP}}{T_F}\right) - 3.539 \log\left(\frac{W}{T_F}\right) \qquad (5\text{-}1)$$

developed by Zettlemoyer to predict SCF at cover plate details is modified to

$$SCF = 5.798 + 1.981 \log\left(\frac{1}{\frac{T_F}{T_{CP}}}\right) - 3.539 \log\left(\frac{W}{T_{CP}} \times \frac{1}{\frac{T_F}{T_{CP}}}\right) \qquad (5\text{-}2)$$

and plotted for both values of W/T_{CP} as a comparision. Plotted results from each method are very close in both shape and magnitude considering that Equation 5-1 is being extrapolated beyond the T_F/T_{CP} range from which it was developed.

5.3 Comparison to SPATE Results

Stress concentration factors have also been obtained experimentally by measuring stresses at a cover plate detail

using the SPATE (Stress Pattern Analysis by Thermal Emission) technique[15]. The test was conducted on an axially loaded tension member with a 1 in. flange, 5/8 in. cover plate and 0.4± in. fillet weld at the Alcoa Technical Center facilities. Stresses measured by this technique are a summation of the principal stresses over a spot resolution area of 0.028 in. x 0.028 in. and yield a SCF of 1.8-1.9 for the tension specimen.

To make an accurate comparison between SCF's determined by the SPATE technique and finite element analysis, the mesh size at the toe of the fillet weld must be equivalent to the spot resolution area. Results from submodel 2 for the tension specimen with $W/T_{CP}=0.64$ and $T_F/T_{CP}=1.6$ which has a mesh size of 0.025 in. x 0.025 in. is used for the comparision. However, since the mesh size is smaller than 0.028 in. the calculated SCF of 2.8 is approximately 50% higher than the SPATE results. Based on a linear interpolation relating SCF to mesh size, approximately 50% of this discrepancy can be contributed to the 0.003 in. difference in measuring size. Future comparisions should be done without any size differential between methods.

Chapter 6 - SUMMARY AND CONCLUSIONS

The primary intent of this study has been to develop an analytical model of fatigue crack propagation and life prediction for aluminum cover plate details. Also examined is the effect of cover plate geometry on stress concentration and the effect of cover plate orientation on fatigue life. The more important findings of this report and recommendations for future work are discussed below.

1. Verified that Albrecht and Yamada's procedure to rapidly calculate stress intensity factors provide results which compare closely to values obtained using the Energy Release Rate method to calculate upper-bound solutions at cover plate details. Accurate values of K can be found by using this simple and computer efficient model which requires a single uncracked analysis to determine the distribution of stresses along the crack path. An even more accurate procedure to validate the Green's function results would be for a fully three-dimensional analysis to be performed where K is calculated by the Energy Release Rate method for comparison. Although currently unfeasible because of resource limitations, in the future it may be possible.

2. Developed an analytical model to predict fatigue life at both beam and tension specimen cover plate details for

aluminum alloy 5456-H116. From this model, the following observations can be made regarding the behavior of cover plate details:

A. Tension specimen details have fatigue lives 40% higher than those of beam specimens primarily due to the absence of a bending stress gradient through the flange thickness.

B. Cover plate orientation affects fatigue life. Beam specimens with cover plates extending from each end of the beam towards midspan (current test specimens) exhibit a fatigue life 14% higher than a conventionally oriented detail at the same nominal stress. This 14% difference is for the specific case studied in this report and may vary depending on the details individual parameters.

3. Qualitatively demonstrated that the fatigue strength of cover plate details is a function of more than flange thickness. Rather, the distinction between categories E and E′ should be based on relative detail geometry such as the ratios of T_F/T_{CP} and W/T_{CP}. Future work can expand the parametric study to include beam specimens from which fatigue life values will be calculated. From these generated S-N values, a quantitative relationship can be established to distinguish between categories E and E′ based on the relative cover plate geometry.

Crack Length (in)	Stress Intensity Factor ($ksi\sqrt{in}$)		Percentage Difference
	Uncracked Global Condition	Cracked Global Condition	
0.005	3.91	–	–
0.010	4.45	–	–
0.020	5.01	–	–
0.050	5.73	6.40	11.7
0.100	5.76	7.24	25.7
0.200	5.87	9.44	60.8

Table 1 - Stress Intensity Factors by the Energy Release Rate Method

Stress Range (ksi)	Beam Specimen						Tension Specimen		
	Conventional Cover Plate Orientation			Test Cover Plate Orientation					
	a_i=0.001"	a_i=0.006"	% Diff.	a_i=0.001"	a_i=0.006"	% Diff.	a_i=0.001"	a_i=0.006"	% Diff.
2.9	3,734,000	3,303,000	13.0	4,241,000	3,740,000	13.4	5,294,000	4,600,000	15.1
4.1	1,277,000	1,130,000	13.0	1,451,000	1,279,000	13.4	1,811,000	1,574,000	15.1
5.8	436,000	386,000	13.0	495,000	437,000	13.3	618,000	537,000	15.1

Table 2 - Calculated S-N Data Points

		W/T_{CP}	
		0.64	0.80
T_F/T_{CP}	1.0	6.98	6.49
	1.4	–	7.17
	1.6	7.94	–
	2.0	–	7.82
	2.6	–	8.23
	3.0	8.97	8.43
	4.0	–	8.76

Table 3 - Stress Concentration Factors

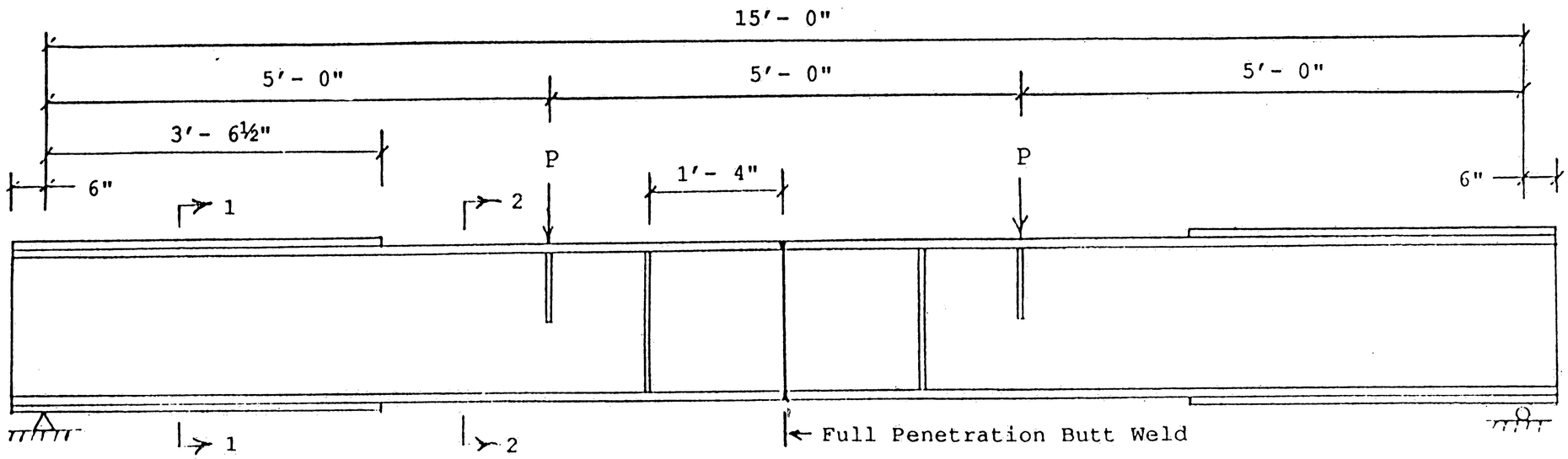

Beam Elevation

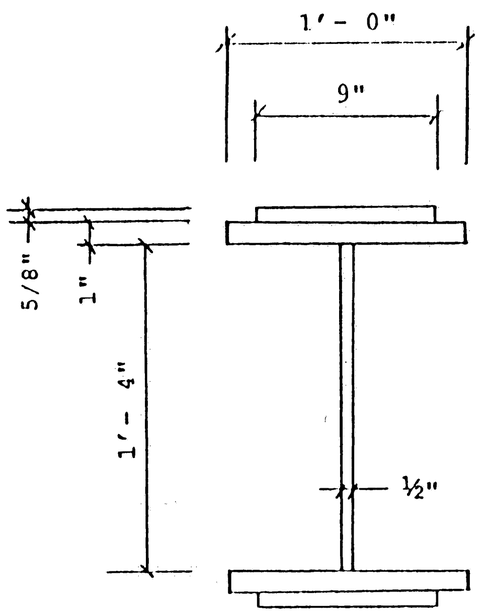

Section 1-1

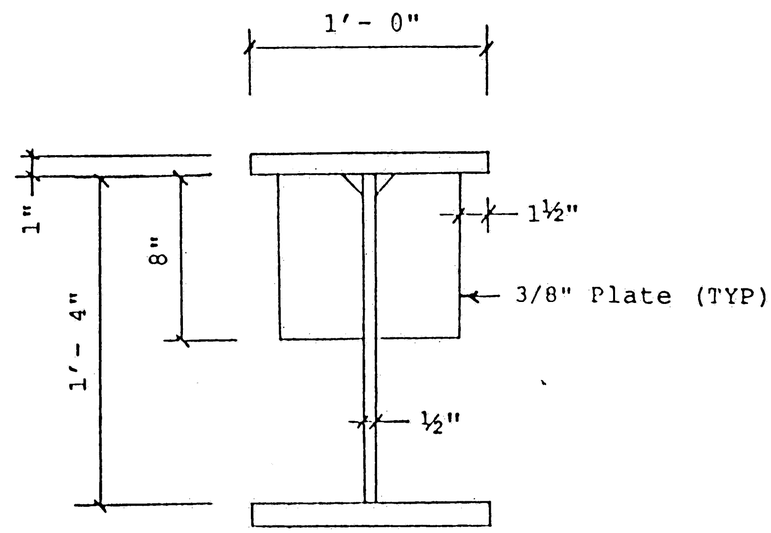

Section 2-2

Figure 1 - Beam Geometry

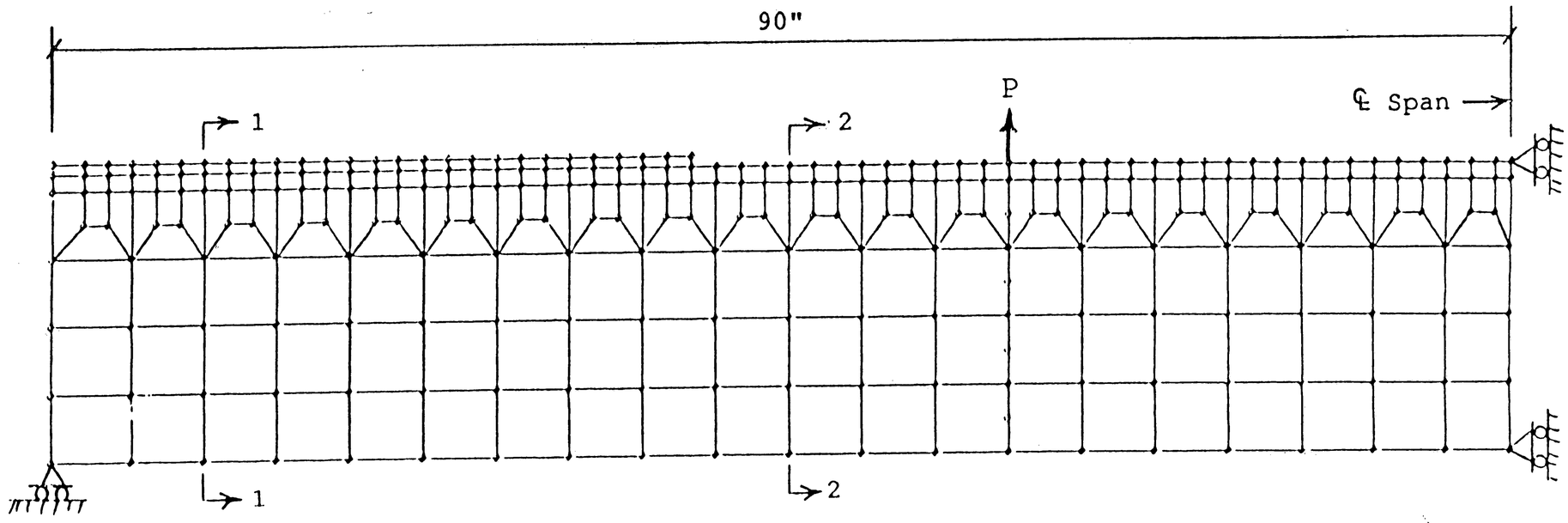

A. Cover Plate Orientation on Test Specimen

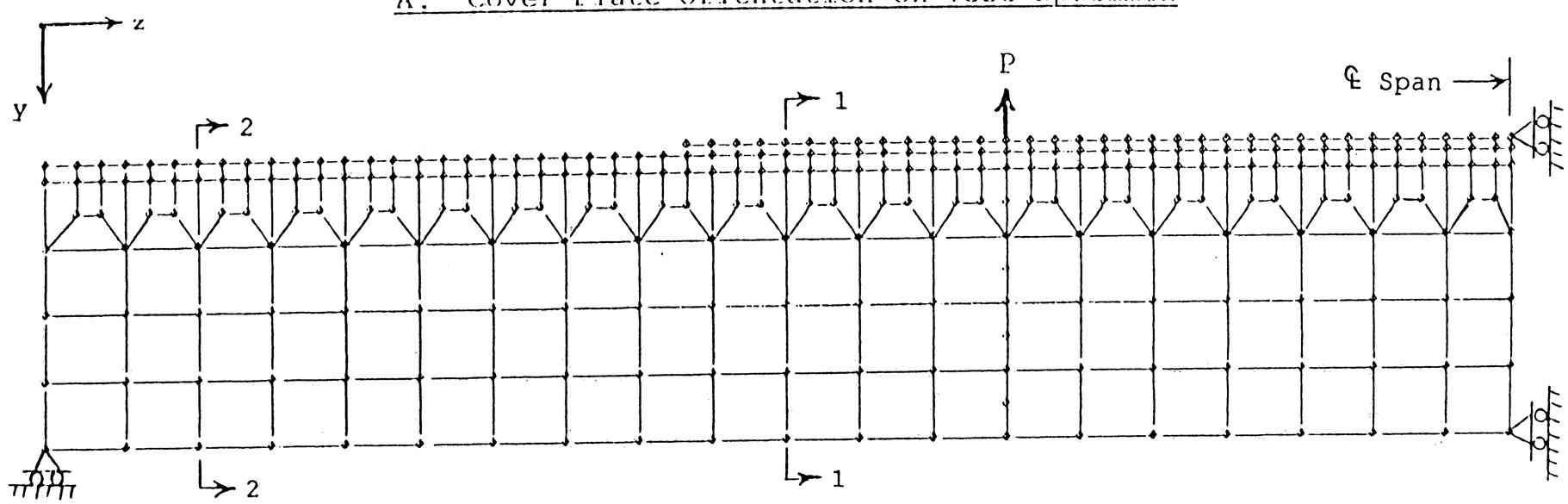

B. Conventional Cover Plate Configuration

Figure 2 - Elevation of 3-D Finite Element Mesh

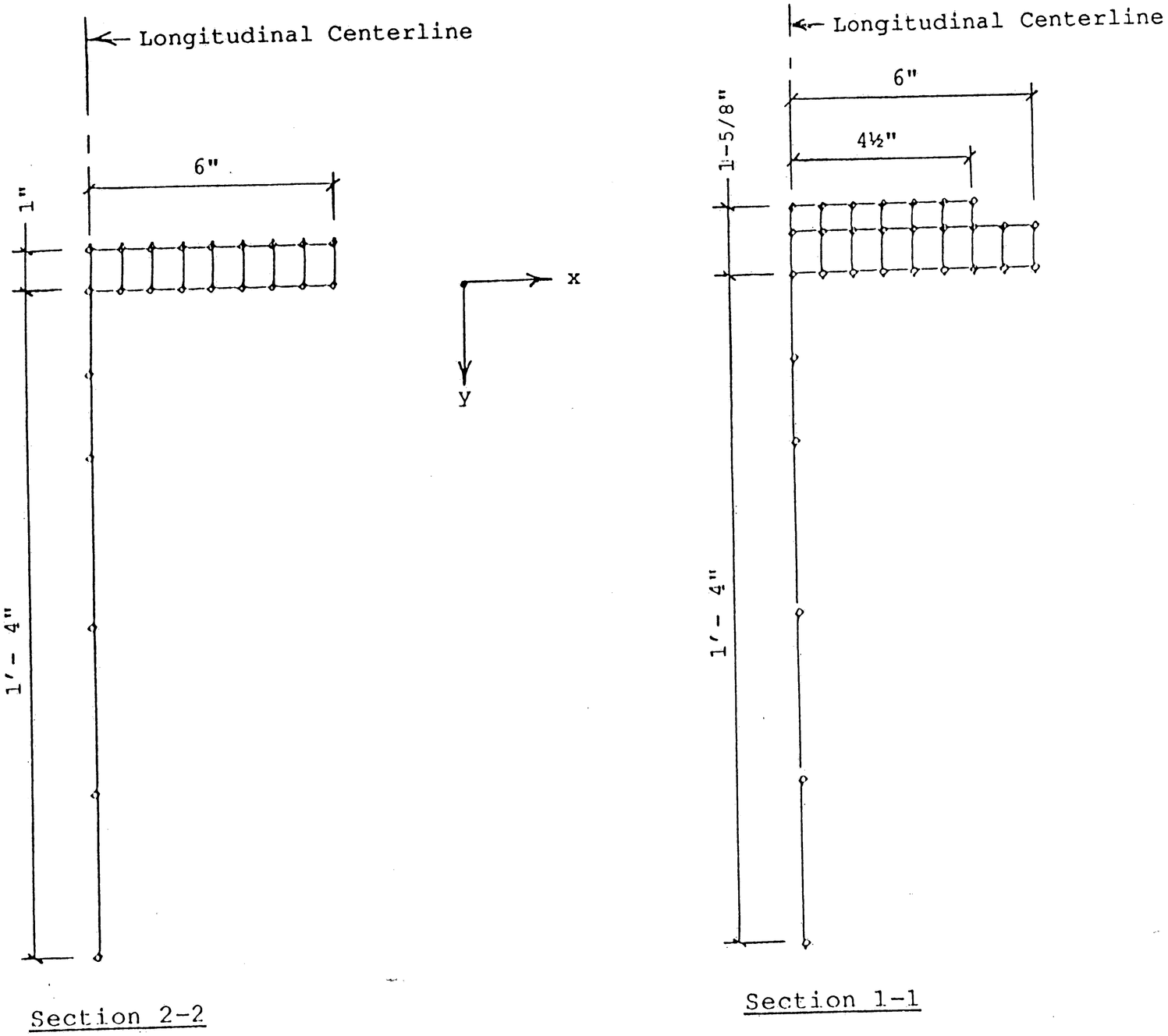

Figure 3 - Cross Section of Finite Element Mesh

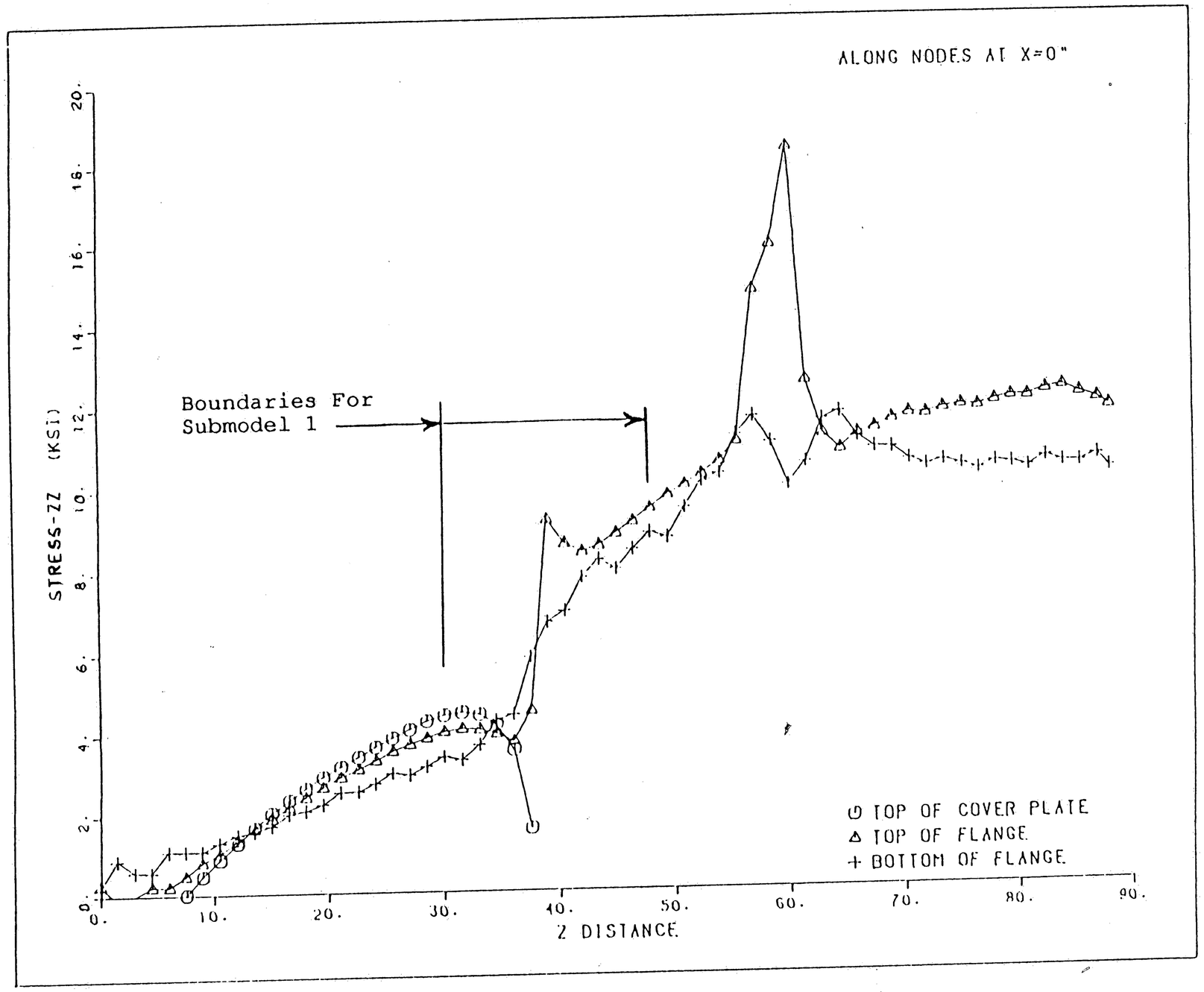

Figure 4 - Beam Flange Stress Distribution along Web Centerline

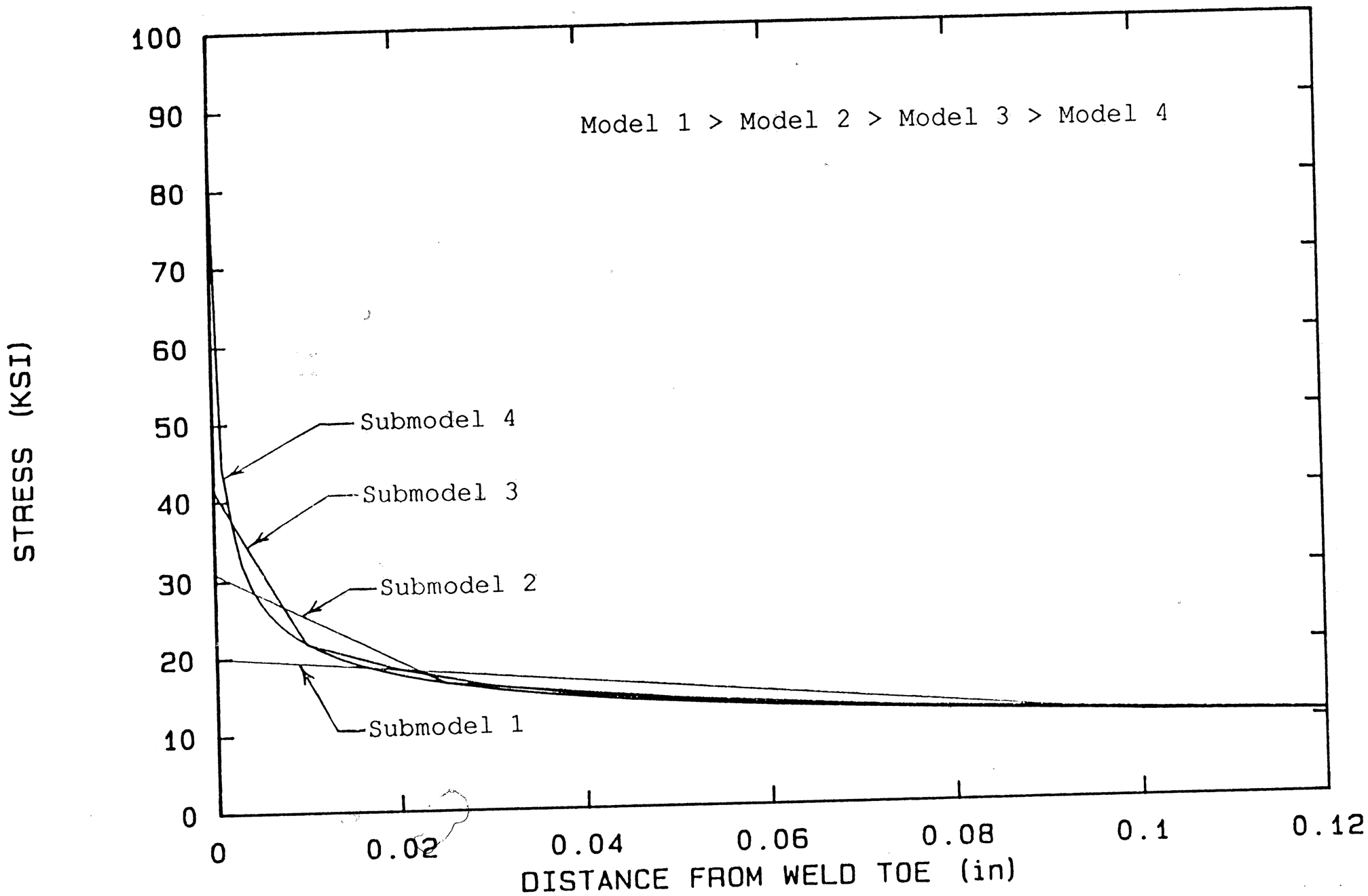

Figure 5 - Influence of Mesh Size on Maximum Stress

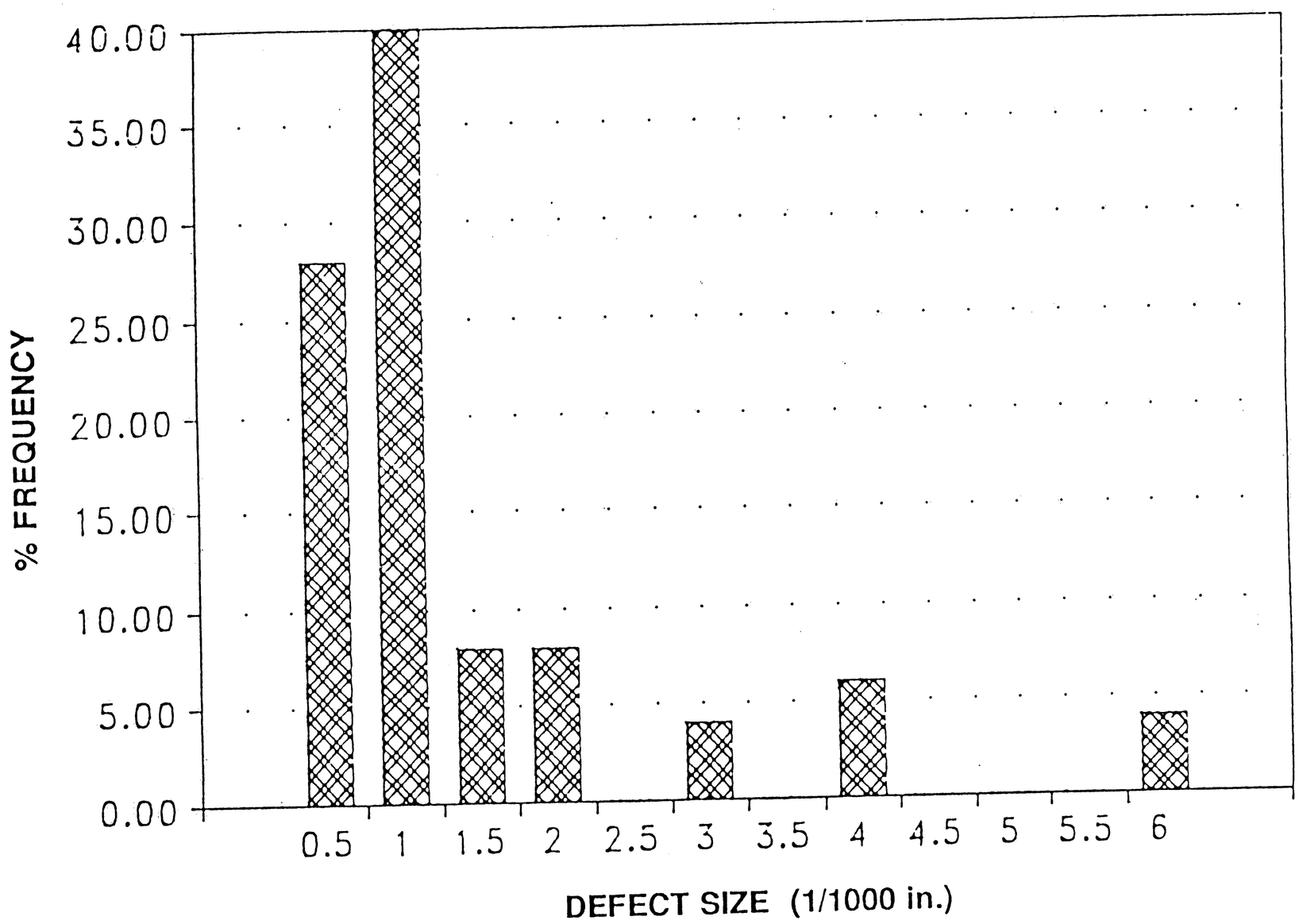

Figure 6 - Partial Histogram of Welded Joint Defect Sizes

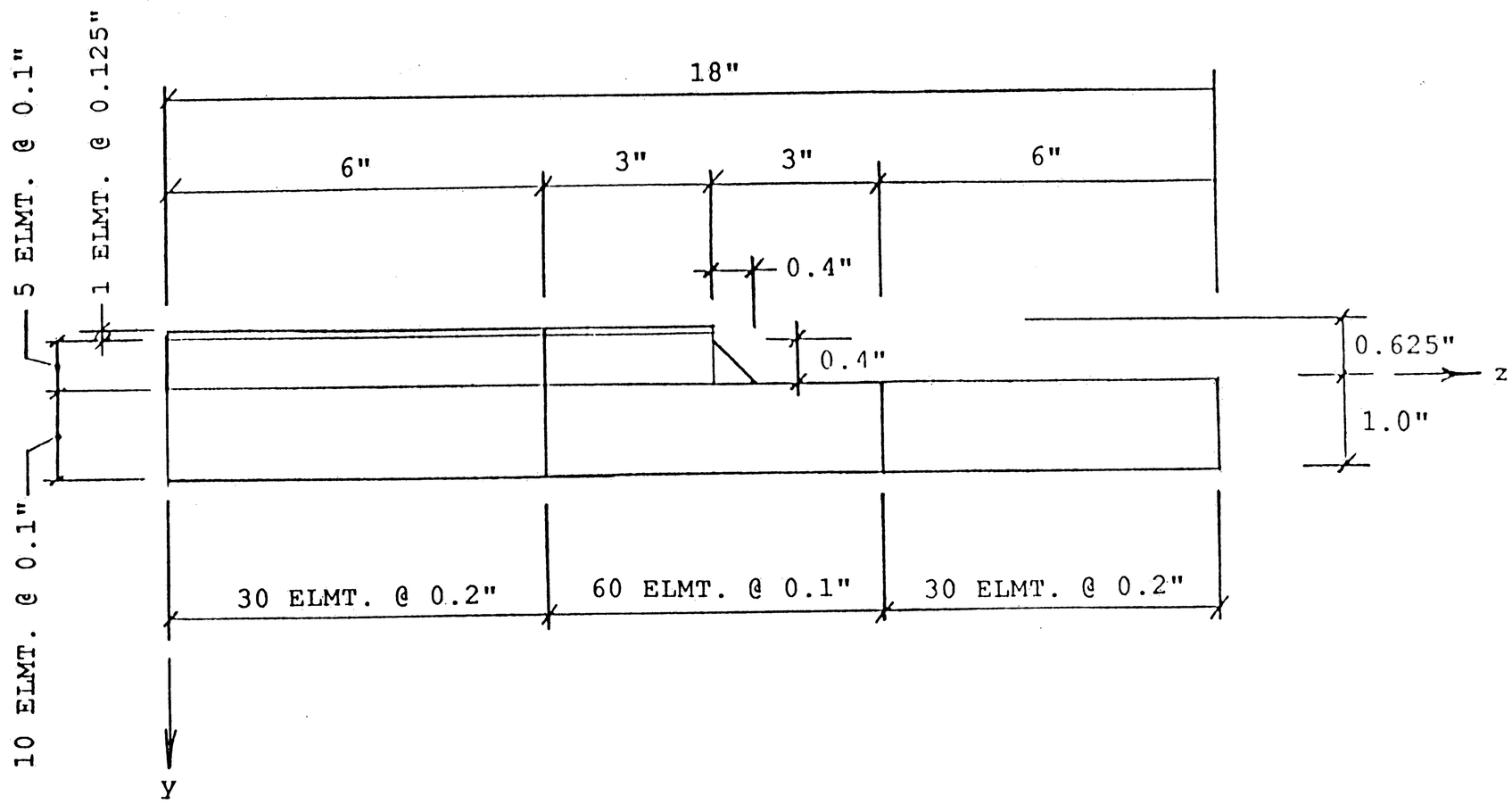

Figure 7 - Submodel 1

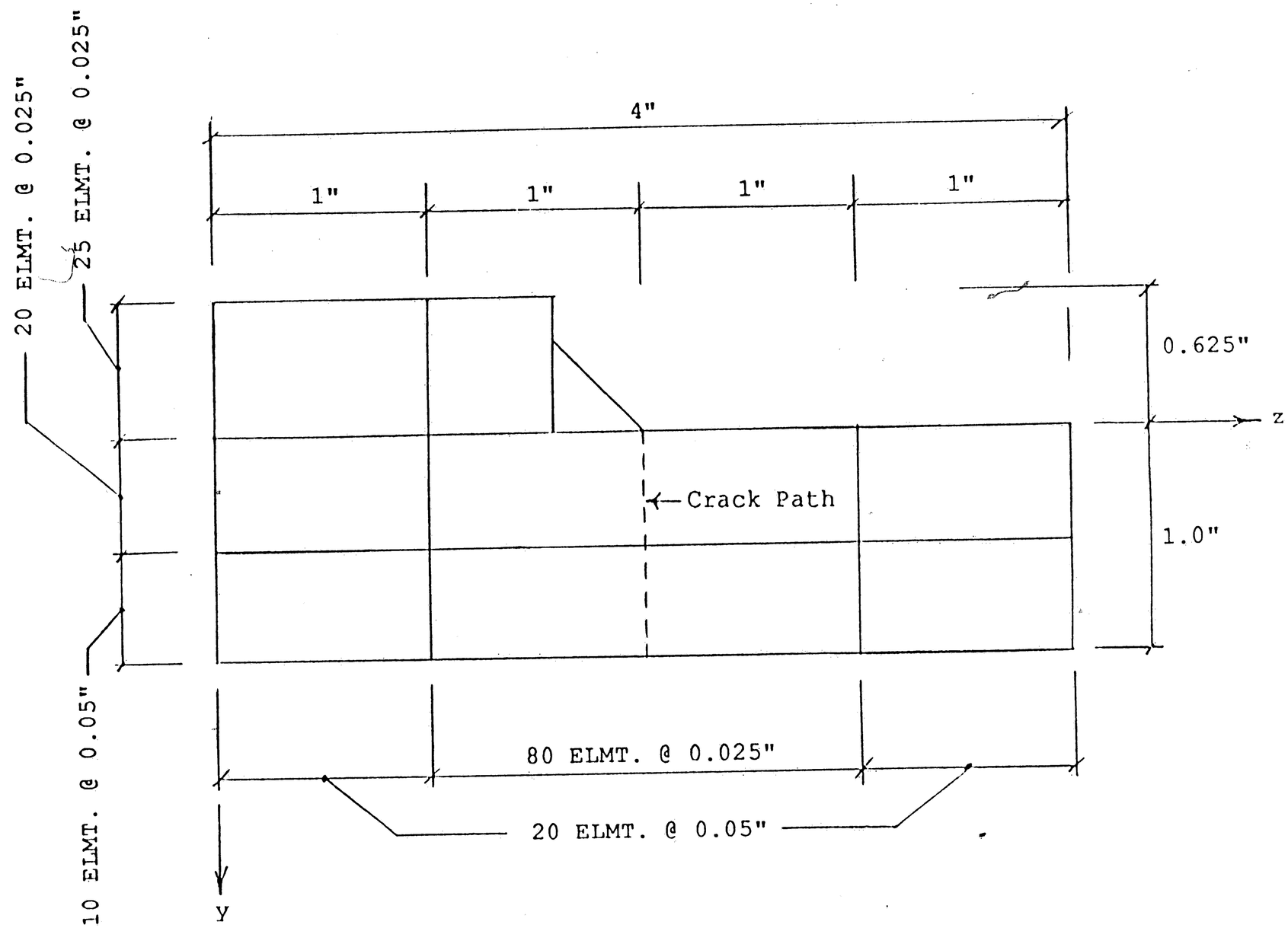

Figure 8 - Submodel 2

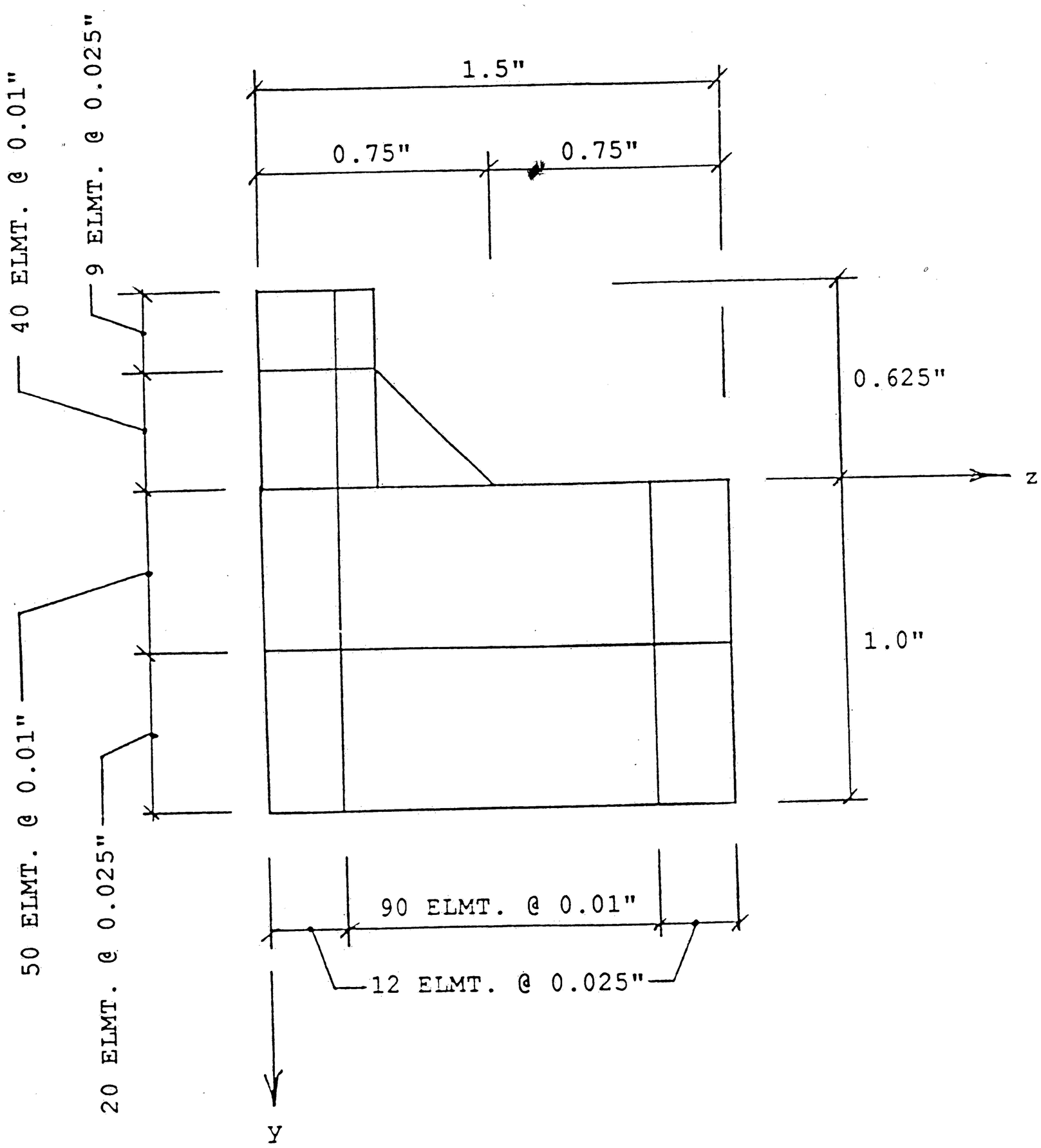

Figure 9 - Submodel 3

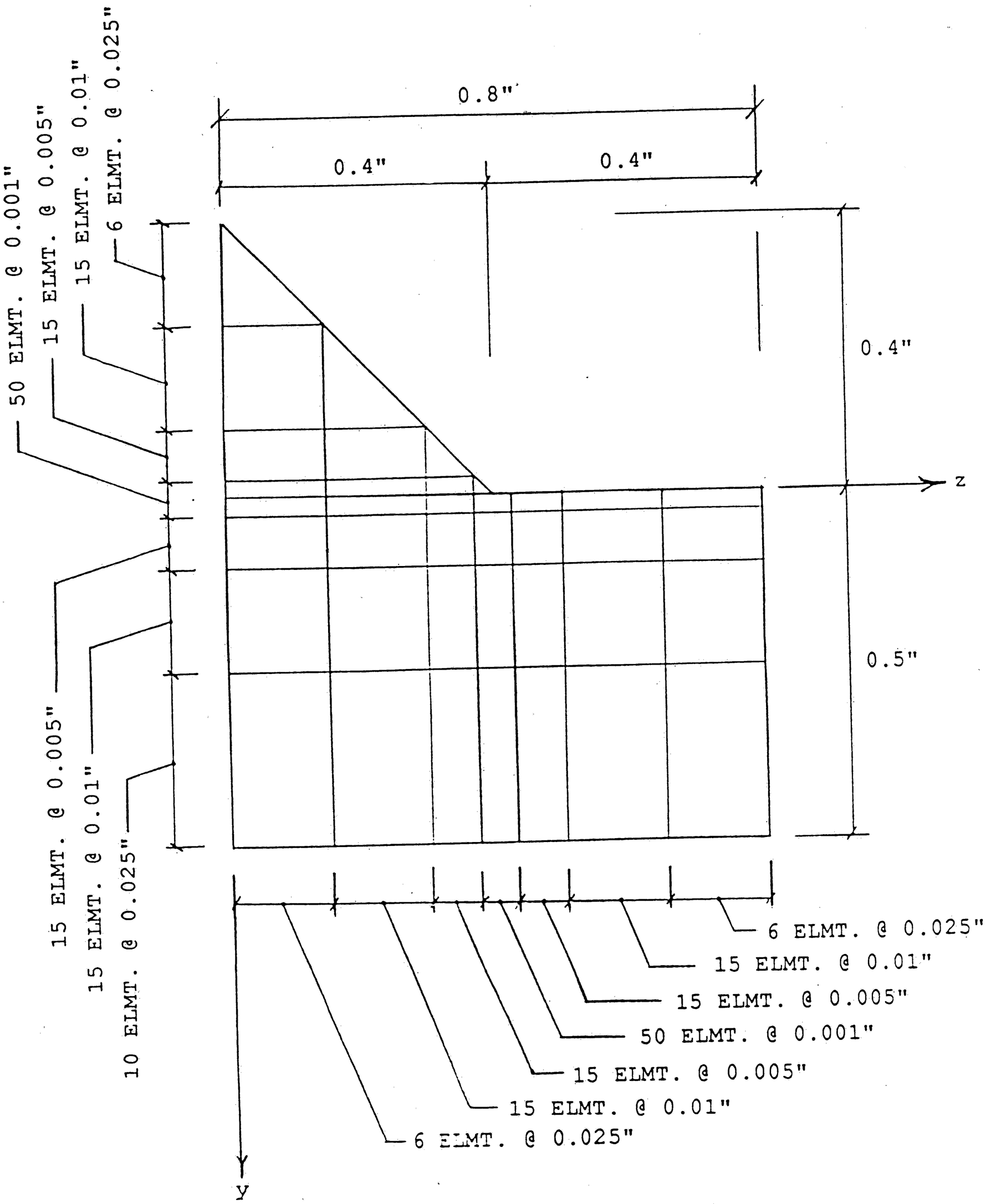

Figure 10 - Submodel 4

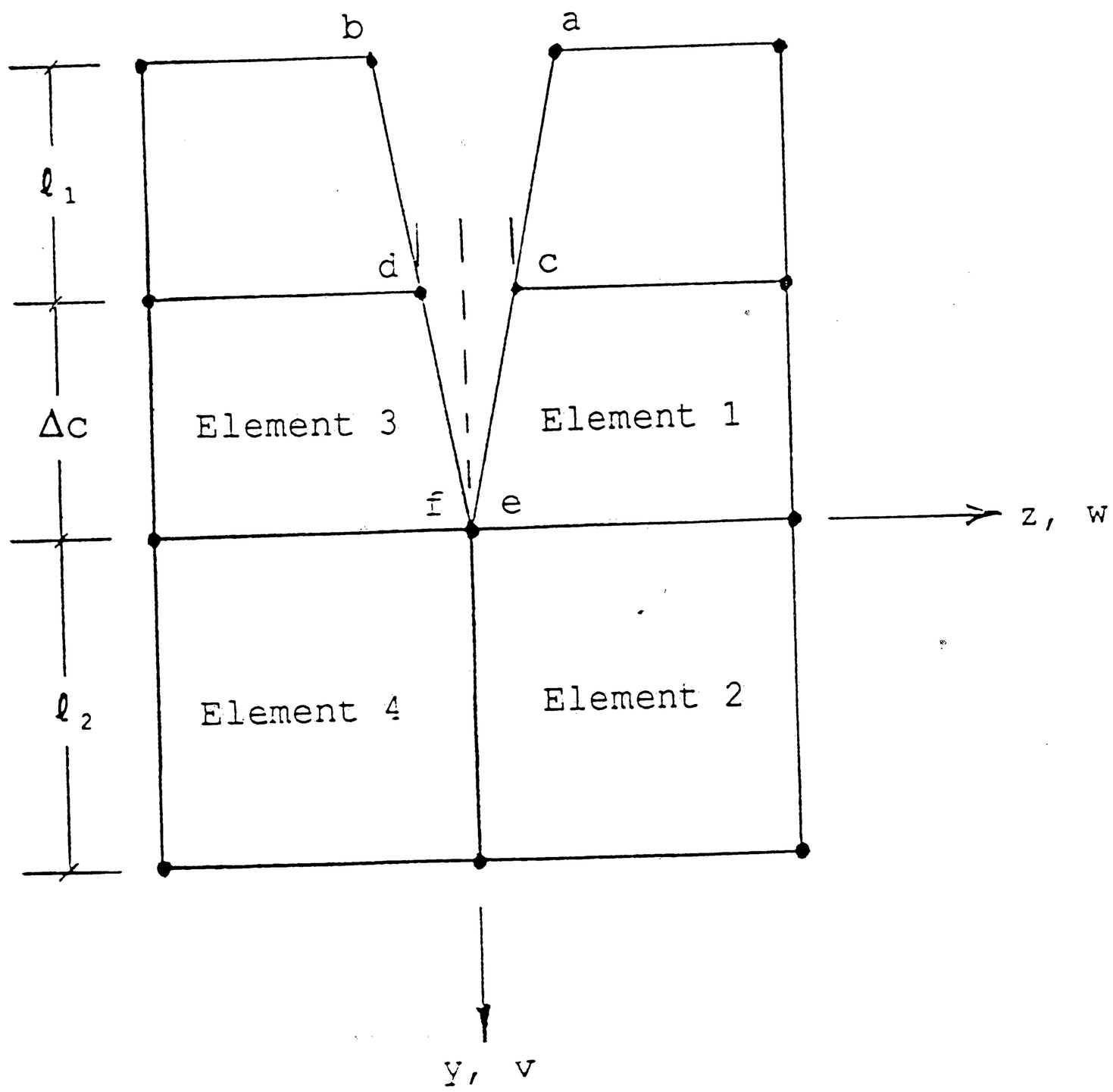

Figure 11 - Finite Element Nodes Near Crack Tip

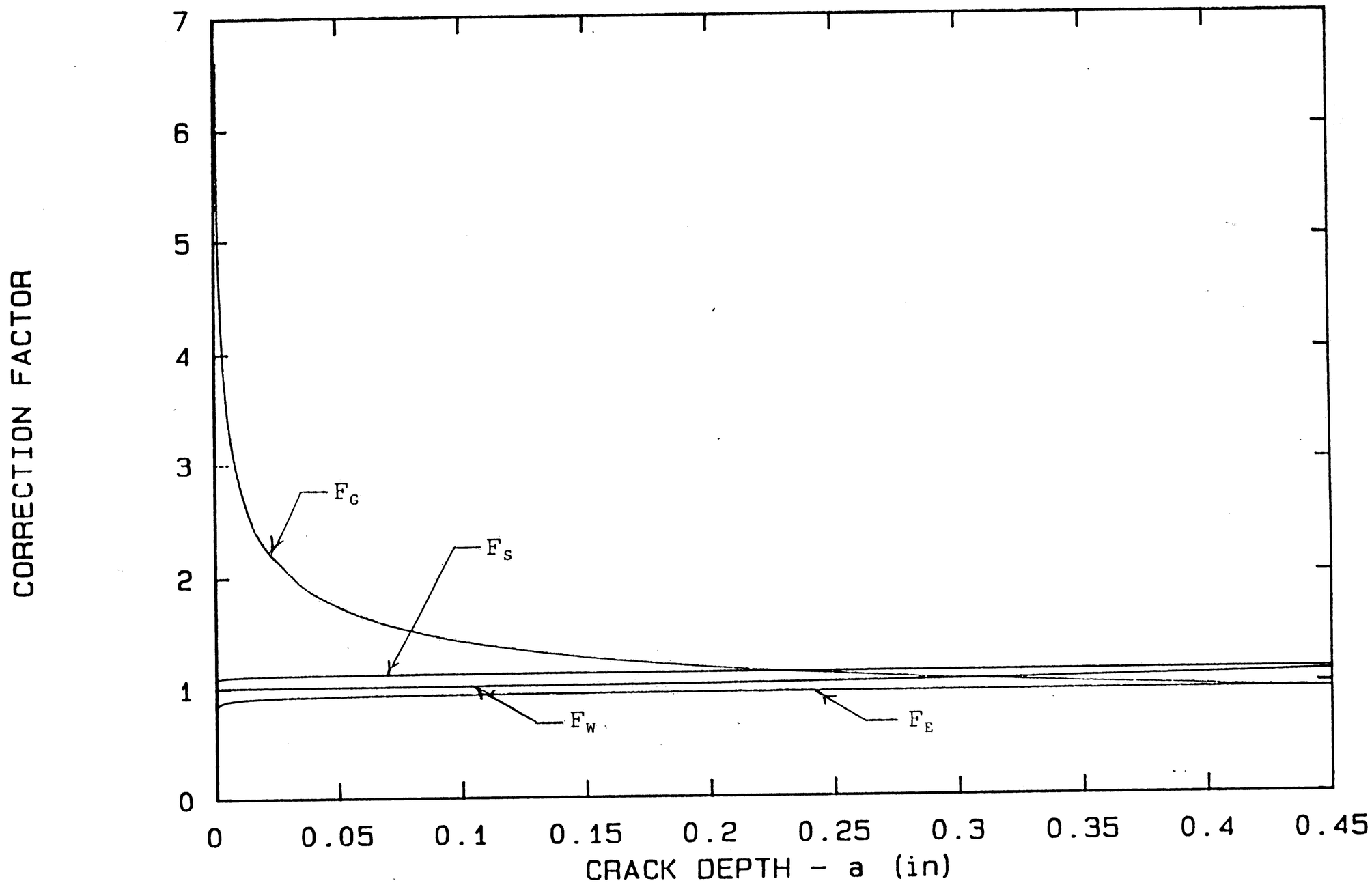

Figure 12 - Correction Factor Variation with Crack Depth

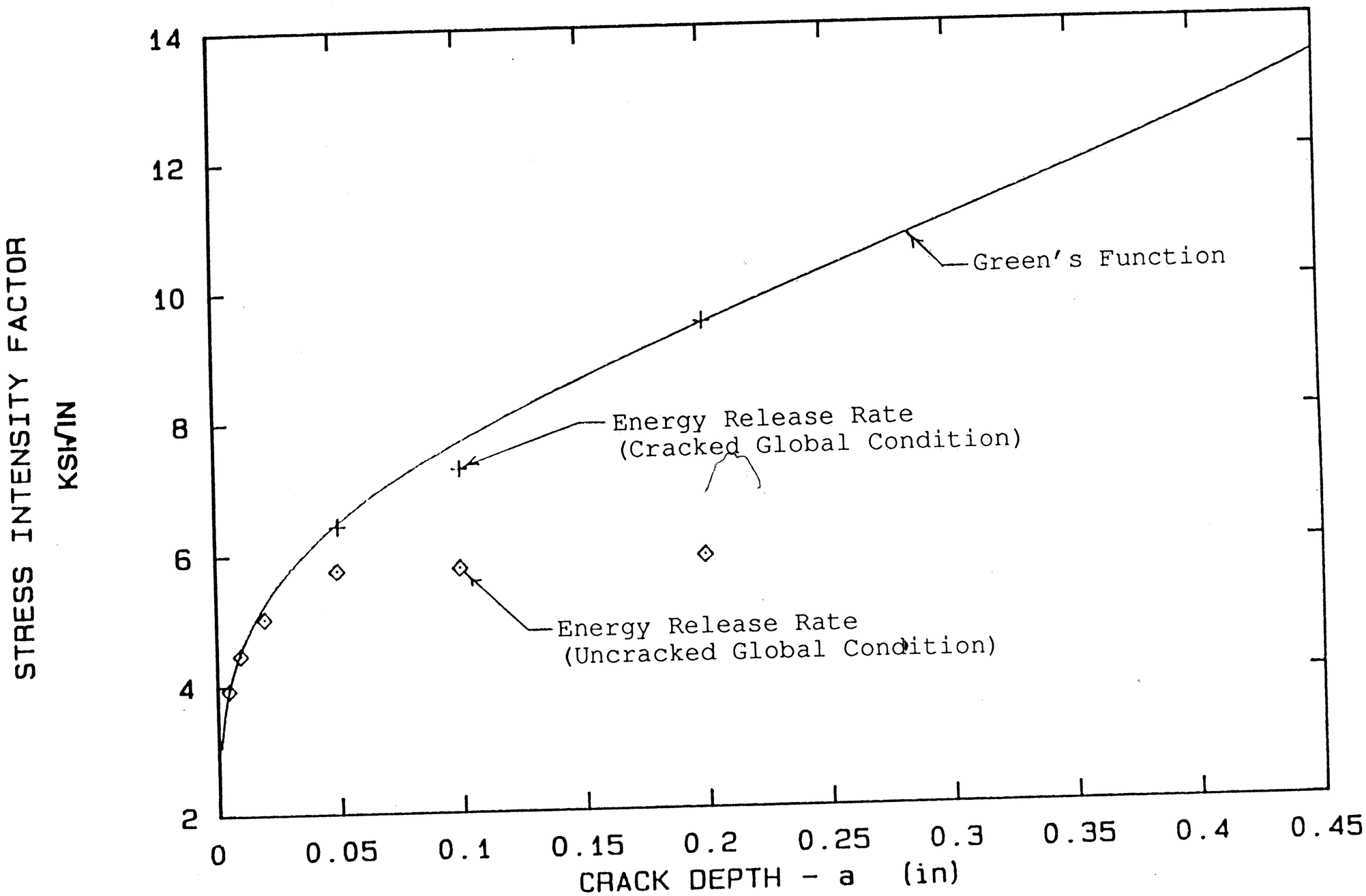

Figure 13 - Calculated Stress Intensity Factors for Tension Specimen

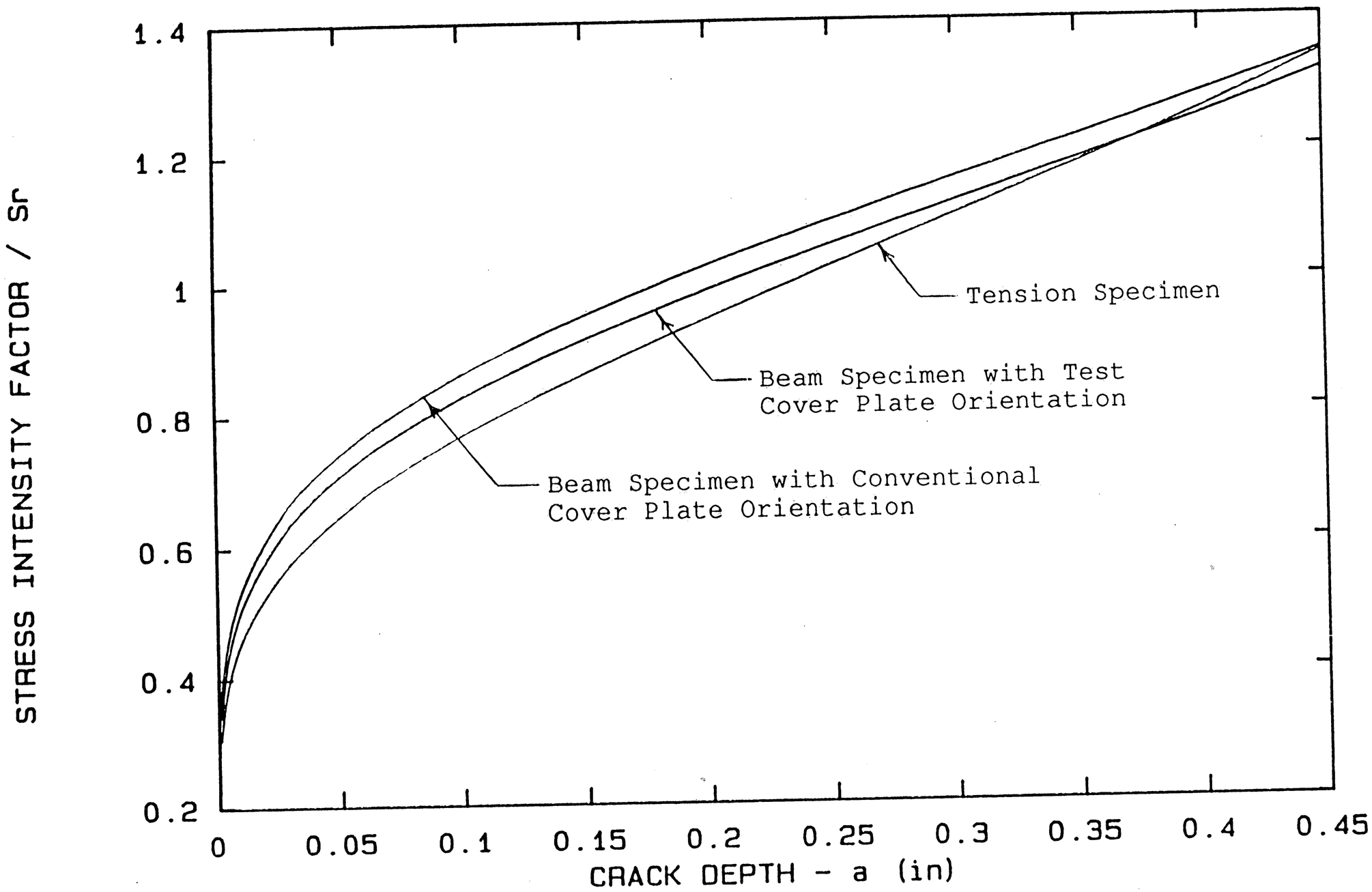

Figure 14 - Stress Intensity Factor Variation with Specimen Type

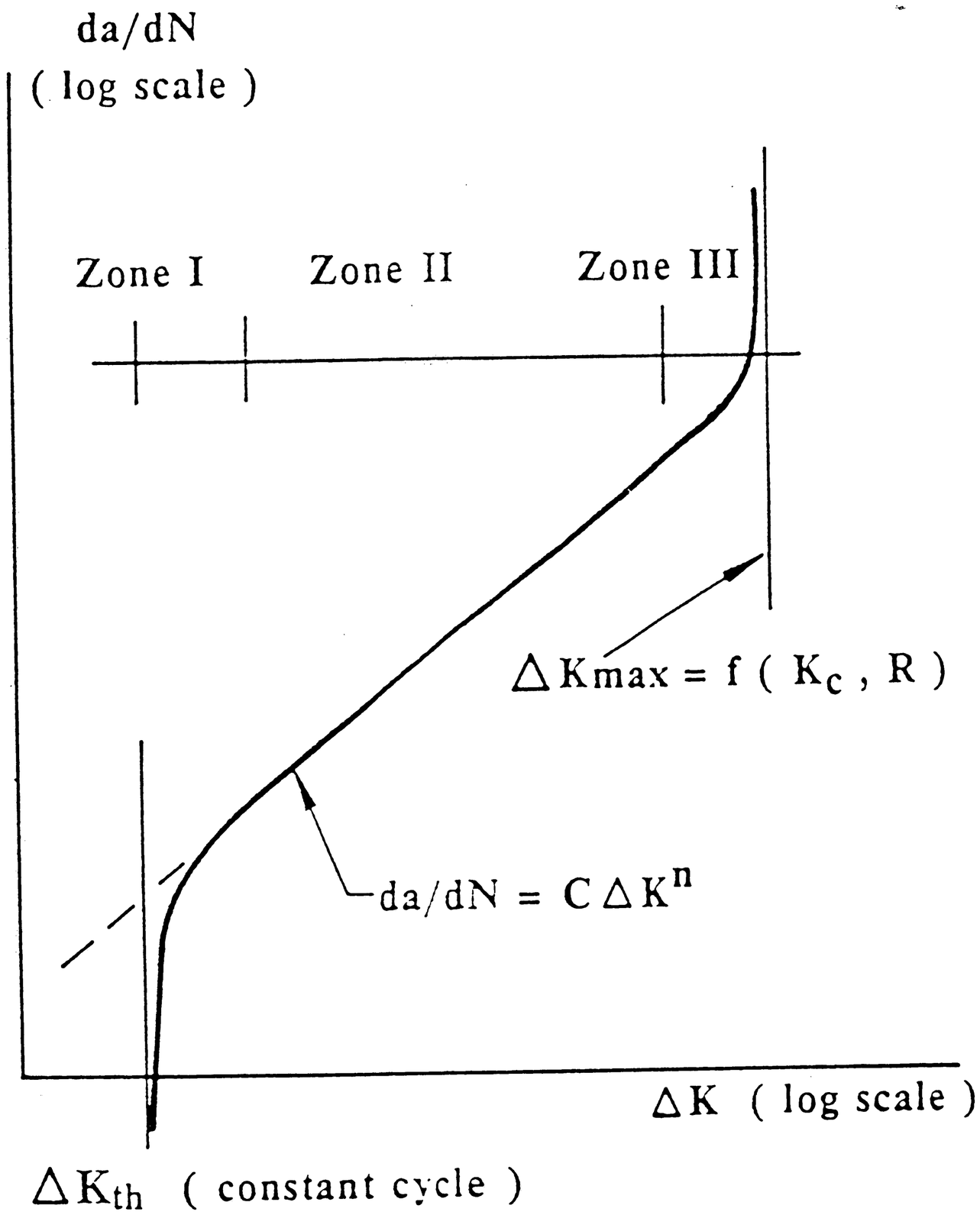

Figure 15 - Fatigue Crack Propagation Curve

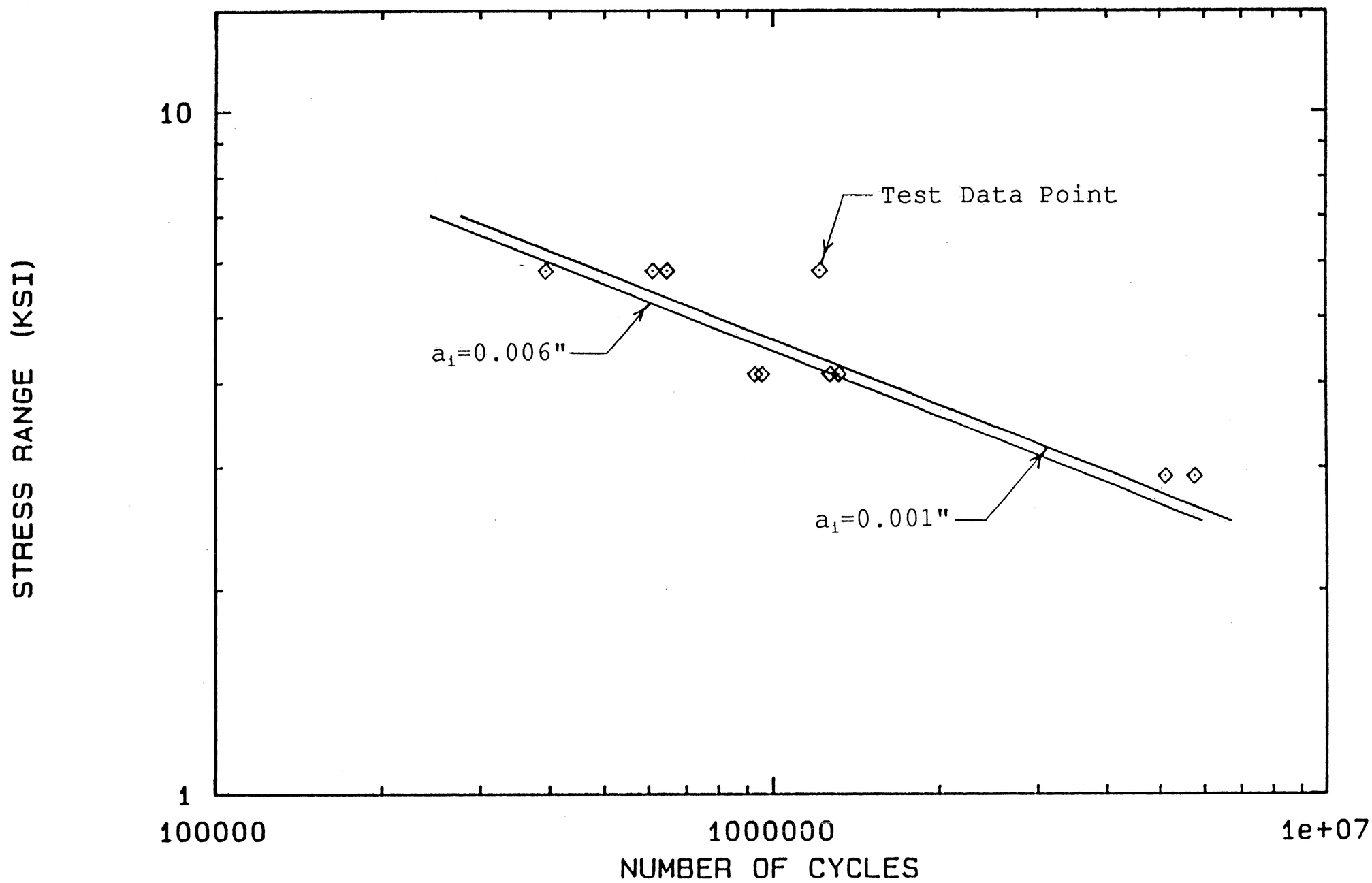

Figure 16 - Generated S-N Curve for Beam Specimen

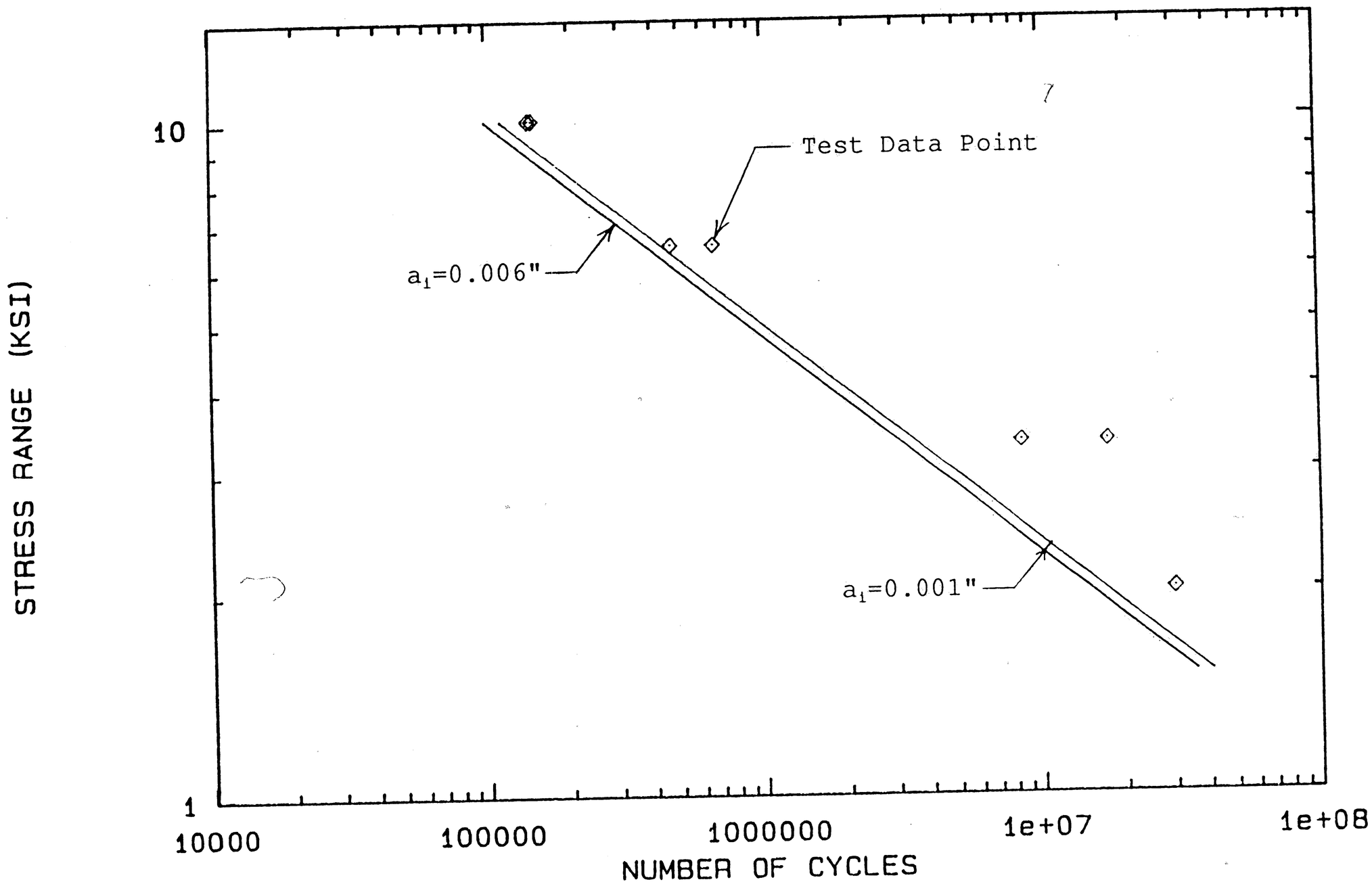

Figure 17 - Generated S-N Curve for Tension Specimen

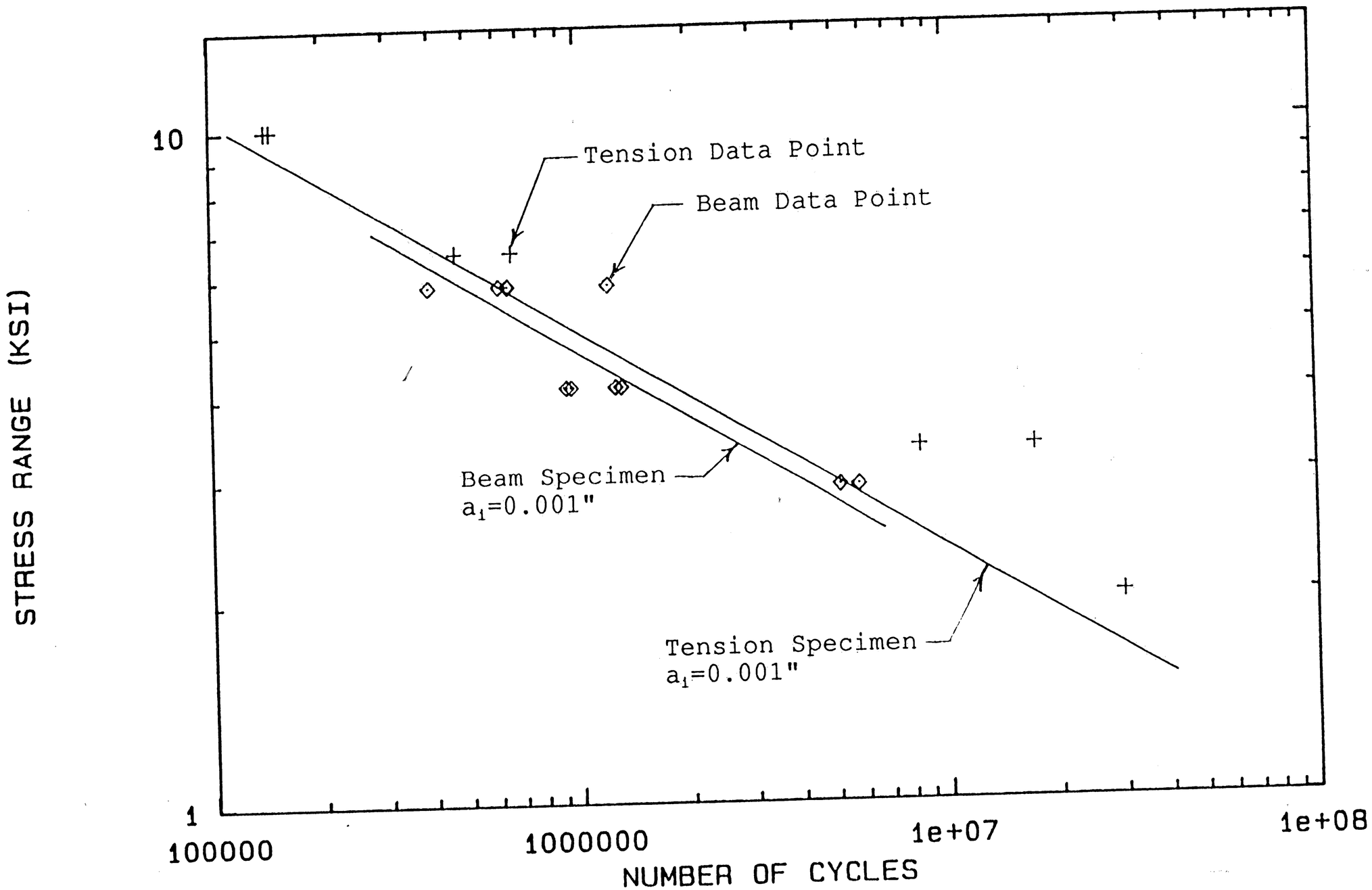

Figure 18 - Combined S-N Curves

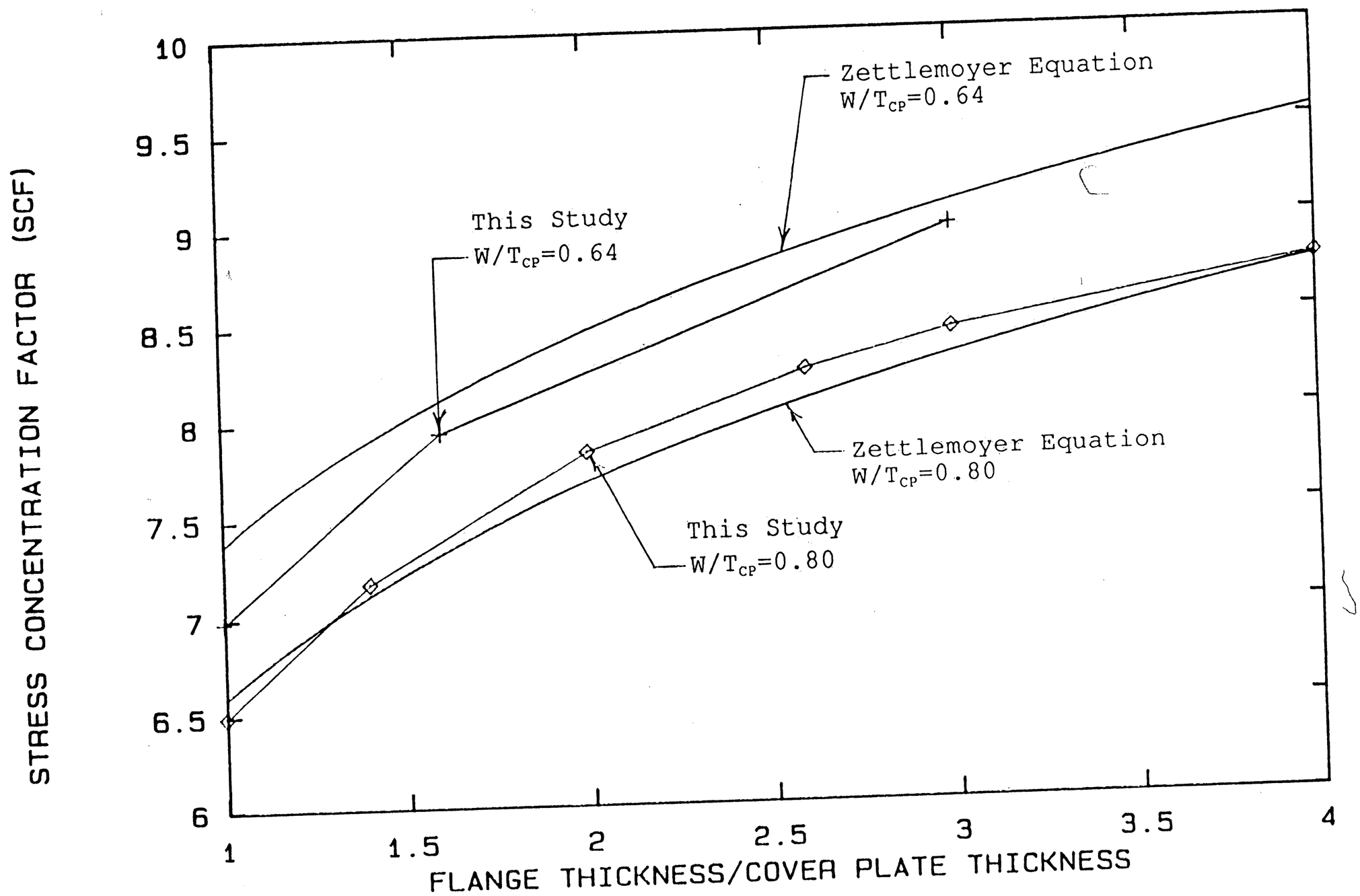

Figure 19 - Stress Concentration Factor Variation

REFERENCES

1. Wohler, A., "Tests to Determine the Forces Acting on Railway Carriage Axles and the Capacity of Resistance of the Axles," *Engineering*, **11** (1871).

2. "The AASHO Road Test Report 4." *HRB Special Report 61D* (1962).

3. Slockbower, R.E. and Fisher, J.W., "Fatigue Resistance of Full-Scale Cover Plated Beams," *Fritz Eng. Lab. Report 386.9*, Lehigh University (July 1978).

4. AASHTO Subcommittee on Bridges and Structures, Interim Specifications Bridges 1974, American Association of State Highway and Transportation Officials, Washington D.C. (1974).

5. Fisher, J.W., Hausammann, H., Sullivan, M.D., and Pense, A.W., "Detection and Repair of Fatigue Damage in Welded Highway Bridges," NCHRP Report 206 (1979).

6. Manual of Steel Construction, 9th edition, American Institute of Steel Construction, Inc., Chicago (1989).

7. AASHTO, American Association of State Highway and Transportation Officials, Standard Specifications for Highway Bridges, 14th edition, Washington, D.C. (1989).

8. Irwin, G.R., "Analysis of Stresses and Strains near the End of a Crack Traversing a Plate," *Transactions, American Society of Mechanical Engineers*, Series E, **24(3)**, (1957).

9. Tada, H., Paris, P.C., and Irwin, G.R., The Stress Analysis of Cracks Handbook, Del Research Corp., Hellertown, PA (1973).

10. ADINA R & D, Inc., ADINA Users Manual, Watertown, MA. (1987)

11. Rybicki, E.F. and Kanninen, M.F., "A Finite Element Calculation of Stress Intensity Factors by a Modified Crack Closure Integral," *Engineering Fracture Mechanics*, **9** (1977).

12. Albrecht, P. and Yamada, K., "Rapid Calculation of Stress Intensity Factors," *ASCE - Journal of the Structural Division*, No. ST2, Paper 12742, February 1977.

13. Zettlmoyer, N., Stress Concentration and Fatigue of Welded Details, PhD Dissertation, Lehigh University (1976).

14. Peterson, R.E., Stress Concentration Factors, J. Wiley and Sons, New York, (1974)

15. Menzemer, C.C., Unpublished Alcoa Project Report, July 1990.

16. Irwin, G.R., Fracture, Handbuch der Physik, **6**, 551 (1958)

17. Newman, J.C., "Review and Assessment of Stress Intensity Factors for Surface Cracks," in Part-Through Crack Fatigue Life Predictions, J.G. Chang, ed., American Society for Testing Materials, 16-42 (1979).

18. Fisher, J.W., Fatigue and Fracture in Steel Bridges, Case Studies, John Wiley and Sons, New York (1984).

19. Paris, P.C. and Erdogan, F., "A Critical Analysis of Crack Propagation," *Journal of Basic Engineering, Transactions*, ASME Series D, **85**, (1963).

20. Kosteas, D., "Aluminum Beam Testing Program - Assessing the Results," International Conference on the Fatigue of Welded Constructions, TWI, Brighton (1987).

VITA

The author was born in Wilkes-Barre, Pennsylvania on February 23, 1961 as the only child of Hermine and Stanley Kaczinski. He graduated from Wilkes-Barre Coughlin High School in 1979 and went on to study at Lafayette College in Easton, Pennsylvania. In May of 1983 he graduated Cum Laude from Lafayette College with a Bachelor of Science Degree in Civil Engineering.

After graduation, the author worked for the consulting engineering firms of Modjeski & Masters, Huth Engineers Inc. and the G. Edwin Pidcock Company as a structural engineer for both bridge and building projects. During this period, the author wed the former Miss Mary S. Bowker of Pittsburgh, PA.

The author entered Lehigh University in August of 1988 to pursue a Master of Science Degree in Civil Engineering. Since that time he has worked as a research assistant on two different projects. The first year he was involved in an analytical study of lateral load distribution characteristics of skewed prestressed concrete bridge systems for the Pennsylvania Department of Transportation. Since September of 1989 he has been involved in fatigue testing of full-scale welded aluminum beam details for the Research Center for Advanced Technology for Large Structural Systems (ATLSS) in conjunction with the Aluminum Company of America (Alcoa).